Highlights:

- Conceptual review of hyporheic zones of rivers as natural anoxic-oxic bioreactors
- Interactions between organohalide respiration and biogeochemical cycling
- Aerobic vinyl chloride mineralisation during hyporheic mixing is conceptualised
- Field experience, challenges and characterisation technologies critically reviewed

Natural attenuation of chlorinated ethenes in hyporheic zones: a review of key biogeochemical processes and in-situ transformation potential

John J. Weatherill [a] *, Siavash Atashgahi [b], Uwe Schneidewind [c], Stefan Krause [d], Sami Ullah [d], Nigel Cassidy [e], Michael O. Rivett [f g]

[a] School of Physical and Geographical Sciences, Keele University, UK. Current address: School of Biology, Earth and Environmental Science, University College Cork, Ireland.

[b] Laboratory of Microbiology, Wageningen University & Research, Stippeneng 4, 6708 WE Wageningen, The Netherlands.

[c] Department of Engineering Geology and Hydrogeology, RWTH Aachen University, Aachen, Germany.

[d] School of Geography, Earth and Environmental Science, University of Birmingham, UK.

[e] School of Engineering, University of Birmingham, UK.

[f] Department of Civil and Environmental Engineering, University of Strathclyde, Glasgow, UK.

[g] GroundH_2O plus Ltd., Quinton, Birmingham, UK.

* Corresponding author: John Weatherill, School of Biology, Earth and Environmental Science, University College Cork, Ireland. Email: john.j.weatherill@gmail.com.

Abstract

Chlorinated ethenes (CEs) are legacy contaminants whose chemical footprint is expected to persist in aquifers around the world for many decades to come. These organohalides have been reported in river systems with concerning prevalence and are thought to be significant chemical stressors in urban water ecosystems. The aquifer-river interface (known as the hyporheic zone) is a critical pathway for CE discharge to surface water bodies in groundwater baseflow. This pore water system may represent a natural bioreactor where anoxic and oxic biotransformation process act in synergy to reduce or even eliminate contaminant fluxes to surface water. Here, we critically review current process understanding of anaerobic CE respiration in the competitive framework of hyporheic zone biogeochemical cycling fuelled by in-situ fermentation of natural organic matter. We conceptualise anoxic-oxic interface development for metabolic and co-metabolic mineralisation by a range of aerobic bacteria with a focus on vinyl chloride degradation pathways. The superimposition of microbial metabolic processes occurring in sediment biofilms and bulk solute transport delivering reactants produces a scale dependence in contaminant transformation rates. Process interpretation is often confounded by the natural geological heterogeneity typical of most riverbed environments. We discuss insights from recent field experience of CE plumes discharging to surface water and present a range of practical monitoring technologies which address this inherent complexity at different spatial scales. Future research must address key dynamics which link supply of limiting reactants, residence times and microbial ecophysiology to better understand the natural attenuation capacity of hyporheic systems.

Keywords: Chlorinated ethenes, hyporheic zone, natural attenuation, biogeochemistry, biotransformation, heterogeneity.

Abbreviations:

1,1,1-TCA: 1,1,1-trichloroethane; DCA: 1,2-dichloroethane; Ac: acetate, CA: chlorinated ethane; cDCE: *cis*-1,2-dichloroethene; CE: chlorinated ethene; Da: Damköhler number; DIC: dissolved inorganic carbon; DNAPL: dense, non-aqueous phase liquid; DOC: dissolved organic carbon; DOM: dissolved organic matter; DON: dissolved organic nitrogen; HCB: hexachlorobenzene; HCE: higher chlorinated ethene; HFC: hyporheic flow cell; K: saturated hydraulic conductivity; LCE: lower chlorinated ethene; OHR: organohalide respiration; OHRB: organohalide-respiring bacteria; OM: organic matter; PCE: tetrachloroethene; PCR: polymerase chain reaction; POM: particulate organic matter; SCFA: short chain fatty acid; SOM: sedimentary organic matter; TCE: trichloroethene; TCM: trichloromethane; TEA: terminal electron acceptor; TEAP: terminal electron accepting process; VC: vinyl chloride.

1 Introduction

Legacy soil and groundwater contamination by chlorinated ethenes (CEs) remains a global environmental concern (Burston et al., 1993; Jackson, 1998; Rowe et al., 2005; Rivett et al., 2006, 2012; 2014). The higher CEs (HCEs), tetrachloroethene (PCE) and trichloroethene (TCE) are parent compounds employed historically as non-polar solvents for industrial cleaning and degreasing applications which enter aquifers as dense, non-aqueous phase liquids (DNAPLs) (Pankow and Cherry, 1996; Rivett et al., 2014) and release dissolved-phase plumes (e.g. Benker et al., 1996; Rivett and Feenstra, 2005; Koch and Nowak, 2015). Diffusive retention of HCEs in low-permeability and fractured formations is increasingly recognised as an important driver of plume longevity from the resulting back-diffusive flux (Parker et al., 1994; Seyedabbasi et al., 2012; Damgaard et al., 2013; Yang et al., 2014). Under predominantly anoxic conditions, HCEs are reductively transformed to the lower CEs (LCEs) *cis*-1,2 dichloroethene (cDCE) and vinyl chloride (VC) (Squillace and Moran, 2007; Chambon et al., 2010; Huang et al., 2014; Lu et al., 2015). CEs have been detected in surface water with alarming frequency around the world (e.g. Christof et al., 2002; McGuire et al., 2004; Ellis and Rivett, 2007; Yamamoto et al., 2014 Wittlingerová et al., 2016). Groundwater baseflow input of CEs has been implicated as a contributory factor in the global impoverishment of surface water ecological quality

known as urban stream syndrome (Meyer et al., 2005; Roy and Bickerton, 2011; Roy et al., 2017). The aquifer-river interface, inclusive of the hyporheic zone (Fig. 1) forms a key diffuse pathway for discharge of groundwater plumes hydrologically connected with local surface water bodies (Table 1) (Conant et al., 2004; Chapman et al., 2007; McKnight et al., 2012; Weatherill et al., 2014; Puigserver et al., 2014; Simsir et al., 2017; Sonne et al., 2017).

The hyporheic zone of streams and rivers has been defined by various disciplines from alternative perspectives (e.g. Boulton et al., 1998; Buss et al., 2009; Krause et al., 2011; Cardenas, 2015). In this review, we conceptualise the hyporheic zone as a dynamic volume of the saturated zone where the pore water domain is physically influenced by exchanges across the sediment–water interface (Cardenas, 2009). This spatially and temporally variable volume may encompass shallow benthic sediments and adjacent parts of the alluvial aquifer (Boano et al., 2014). The transition zone is frequently heterogeneous with a wide range of saturated hydraulic conductivities (K) and associated scaling of solute residence times (Haggerty et al., 2002; Sawyer and Cardenas, 2009; Gomez-Velez et al., 2014). Fluvial sediments are sites of organic matter (OM) retention with high interstitial surface area linked to enhanced microbial metabolic activity and characterised by sharp physical and biogeochemical gradients (Krause et al., 2013, 2014; Boano et al., 2014; Atashgahi et al., 2015; Narango et al., 2015; Briggs et al., 2016). A generic scenario is depicted in Fig. 1 where OM present in the sediment sequence induces anoxia along discharging groundwater flow paths through the interface. The CE plume depicted may be composed solely of parent HCEs (e.g. McKnight et al., 2010) or a mixture of LCEs (e.g. Sonne et al., 2017; Rønde et al., 2017). Shallow oxic zones are created where local hyporheic exchange flows with the river penetrate the underlying anoxic zone (Hester et al., 2013; 2017, Trauth et al., 2014). Heterotrophic biogeochemical cycling of carbon, nitrogen, sulfur and metals will take place along anoxic sediment flow paths (Baker et al., 2000; Mermillod-Blondin et al., 2005; Lautz and Fanelli, 2008; Rahimi et al., 2015). Fluvial sediments can form niche environments for anaerobic biotransformation of CEs by reductive dechlorination and much interest has arisen in their intrinsic capacity to assimilate groundwater CE loads in baseflow (Table 1) (Conant et al., 2004; Abe et al., 2009; Hamonts et al., 2009; Weatherill et al., 2014; Atashgahi et al., 2015; Freitas et al., 2015; Simsir et al., 2017). Discharging

92 groundwater flow paths through fluvial sediments may enter into mixing zones around infiltrating
93 surface water during hyporheic exchange flows (Boano et al., 2014; Gomez-Velez et al., 2014; Hester
94 et al., 2017). Dynamic pore water oxygen (O_2) gradients are induced in mixing zones as a result (Trauth
95 et al., 2014; Vieweg et al., 2015; Cardenas et al., 2016). These mixing zones provide a separate niche
96 environment for aerobic mineralisation of LCE daughter products originating in the anoxic zone or in
97 partially dechlorinated plumes (e.g. Rønde et al., 2017). Hence, hyporheic zones of groundwater-fed
98 rivers may constitute a unique natural 'biobarrier' for complementary anaerobic and aerobic biological
99 treatment of diffuse baseflow CE pollution (Hamonts et al., 2007; Abe et al., 2009; Atashgahi et al.,
100 2017a; Simsir et al., 2017).

101 The aim of this review is to provide a critical evaluation of the current understanding of
102 synergistic anoxic-oxic biotransformation processes and their environmental supporting conditions in
103 typical riverbed sediment sequences. We consider the fate of parent HCEs in anaerobic heterotrophic
104 food webs driven by OM fermentation and observed metabolic interactions with key biogeochemical
105 cycles. We conceptualise the development of anoxic-oxic interfaces in surface water mixing zones
106 which support aerobic bacteria capable of assimilating LCEs via metabolic and cometabolic pathways
107 with a particular focus on VC. We discuss challenges in integrating microbially-mediated transformation
108 processes occurring in sediment biofilms with larger scale hydrological fluxes observable at field scale.
109 We critically review available in-situ monitoring technologies and support our discussions with insights
110 from recent field experience. This process-based understanding is intended to underpin the risk-based
111 management of legacy CE contamination. The coupled biogeochemical and transport processes
112 understanding is highly relevant for river restoration and prospective ecological engineering applications
113 aimed at reducing the impact of organohalide stressors in urban streams (e.g. Lawrence et al., 2013;
114 Rasmussen et al., 2016; Roy et al., 2017).

115 ## 2 Biotransformation of chlorinated ethenes in riverbed sediments

116 Biotransformation of CEs in hyporheic zones will occur when requisite bacteria, a circumneutral
117 pH, nutrients and electron donors/acceptors are present and where solute residence time equals or
118 exceeds the transformation timescale (half-life) of the contaminant (Meckenstock et al., 2015). In anoxic

zones, CEs may undergo anaerobic reductive dechlorination (hydrogenolysis) by heterotrophic bacteria where chlorine atoms are sequentially replaced by hydrogen (Fig. 2) in organohalide respiration (OHR) (Vogel et al., 1987; Hug et al., 2013; Leys et al., 2013). LCEs produced by OHR may reach oxic interfaces where metabolic and co-metabolic aerobic pathways lead to complete natural attenuation. This part of our review profiles key advances in the understanding of these synergistic biotransformation process for which hyporheic zones present a unique capacity.

2.1 Organohalide respiration

Under anoxic conditions, CEs are terminal electron acceptors (TEAs) for energy conservation (Fig. 2) during oxidation of an electron donor (usually hydrogen) in the presence of a carbon source (usually acetate) and a nitrogen source (ammonium) (Mohn and Tiedje., 1992; Smidt and de Vos, 2004). OHR is an energy-conserving process where the chemically stable carbon-halide bond of organohalides is unlocked by replacing the halogen atom with hydrogen and liberating it as a halide (Fig. 2) (Maymo-Gatell et al., 1997; McCarty, 1997; Aulenta et al., 2002). The reductive cleavage of carbon-halide bonds is catalyzed by membrane-bound, cobalamin-containing enzymes known as reductive dehalogenases (Bommer et al., 2014). OHR is mediated by organohalide-respiring bacteria (OHRB) belonging to district bacterial groups i.e., *Chloroflex*i, *Proteobacteria* and *Firmicutes* (Atashgahi et al., 2016). Members of the genus *Dehalococcoides mccartyi, Dehalogenimonas* and *Dehalobacter* spp. are restricted to OHR for their metabolism, although fermentative growth is also shown in the latter (Justica-Leon et al., 2014; Lee et al., 2012; Yang et al., 2017). In contrast, *Geobacter*, *Desulfuromonas*, *Anaeromyxobacter*, *Desulfomonile*, *Desulfoluna*, *Desulfovibrio*, *Sulfurospirillum* and *Desulfitobacterium* genera are facultative OHRB with versatile metabolisms including but not restricted to OHR (Maphosa et al., 2010; Atashgahi et al., 2016).

2.2 Potential heterotrophic food webs in anoxic zones

2.2.1 Carbon flow in the hyporheic zone

Dissolved organic matter (DOM) is a key source of electron donors and nutrients for OHR and other heterotrophic terminal electron accepting processes (TEAPs) in hyporheic zones (Pusch and Schwoerbel, 1994; Fischer et al., 2005; Zarnetske et al., 2011; Stegen et al., 2016). Anaerobic DOM mineralisation is coupled to the reduction of TEAs as follows (Donn and Barron, 2013):

147 $DOM + TEA \rightarrow DIC + metabolite + NH_4$

148 Where TEA (in descending potential metabolic energy yield) is $O_2 > NO_3 > PCE > Fe(III) > TCE >$
149 $cDCE > SO_4 > VC > CO_2$, DIC is dissolved inorganic carbon, metabolite is N_2, CO_2, Mn^{2+}, LCEs, Fe^{2+},
150 ethene, ethane, S^{2-}, CH_4 and acetate) and ammonium (NH_4). Biogeochemical cycling and OHR will take
151 place when DOM concentrations exceed the stoichiometric requirements (non-limiting) for each TEAP
152 where the reaction timescales are less than the exposure time along reactive sediment flow paths (Haest
153 et al., 2011; Zarnetske et al., 2012; Abbot et al., 2016). Hyporheic sediments are often enriched in
154 complex organic matter (Fig. 1) derived from allochthonous terrestrial ecosystem (such as soil particles
155 and leaf litter) and anthropogenic sources of dissolved-phase and suspended particulate material (e.g.
156 urban runoff and wastewater discharges) (Stelzer et al., 2014; Atashgahi et al., 2015). The nature of the
157 organic material that accumulates in riverbed sediments may also influence the effective residence time
158 of the plumes through hydrophobic partitioning to sedimentary organic matter (SOM) (Conant et al.,
159 2004; Allen-King et al., 2002; Wang et al., 2013).

160 Anaerobic decomposition of particulate organic matter (POM) is initiated by extracellular
161 hydrolytic enzymes produced by primary fermenters which release soluble DOM components capable
162 of traversing bacterial cell walls (Fig. 2) (Mani et al., 2016). Hydrolysis is frequently the rate-limiting
163 step in sedimentation zones with high POM loading rates, large particle size ranges or where highly
164 polymerised complex POM (e.g. lignin) are present that are not readily degradable (Gavala et al., 2003;
165 Nogaro et al., 2007; Atashgahi et al., 2014). DOM hydrolysis is a source of labile dissolved organic
166 carbon (DOC) and dissolved organic nitrogen (DON) species including organic acids and the soluble
167 oligomers and monomers of proteins and carbohydrates which influence the onset and rate of anaerobic
168 respiration processes (Jakobsen and Postma, 1999; Zarnetske et al., 2011; Mineau et al., 2013; Helton
169 et al., 2015). Groundwater typically contains <0.15 mM of DOC (Lapworth et al., 2009; Chapelle et al.,
170 2012). Of this, the labile fraction represents only 0.5–5% of carbon present which is often below
171 thresholds required for induction of catabolic genes (Egli, 2010). In contrast, hyporheic zone pore water
172 DOC concentrations often exceed 1 mM (e.g. Lewandowski and Nützmann, 2010) of which 10–30% is
173 labile and bioavailable (Baker et al., 1999; Vidon and Hill, 2004; Romani et al., 2006).

2.2.2 Molecular hydrogen

Free dissolved hydrogen (H_2) is produced from internal proton reduction during primary and secondary DOC fermentation (Fig. 2) (Nath and Das 2004; Hallenbeck et al., 2009). H_2 serves as the strict electron donor for known obligate OHRB (such as *D. mccartyi*) as well as many facultative OHRB (Jugder et al., 2016). A generalised reaction for H_2 production during fermentation of DOC is given as follows:

$$DOC + 2H_2O \rightarrow DIC + 2H_2 + SCFA + H^+$$

Where SCFA is a short-chain fatty acid which is discussed in the next section. In anoxic sediment zones, DOC fermentation is a metabolic process utilised by common fermentative bacteria such as *Desulfovibrio* (Walker et al., 2009), *Syntrophomonas* (Sieber et al., 2010), and *Clostridium* (Wu et al., 2012), among others. H_2 is also produced by homoacetogens (Diekert and Wohlfarth, 1994), certain acetoclastic methanogens (Heimann et al., 2007) and *Geobacter* spp. (Loffler and Sanford, 2005). Low extracellular H_2 concentrations are required for DOC fermentation to be energetically favourable. This is often maintained by unique syntrophic interspecies H_2 transfer relationships (Fig. 3) amongst anaerobes which express membrane-bound hydrogenases (Walker et al., 2009; Morris et al., 2013; Sieber et al., 2014; Jugder et al., 2015). As a result, the reaction timescales for H_2 uptake are typically on the order of minutes (Heimann et al., 2009). Under electron-donor limiting conditions, ambient H_2 concentrations in sediments are often at steady-state that is determined by the hydrogenotrophs with the lowest threshold concentration (Lovely and Goodwin, 1988; Fennel et al., 1997; Loffler et al., 1999; Hoelen and Reinhard, 2004). H_2 threshold ranges have been reported for specific TEAPs (Fig. 4) ranging from <0.1 nM for denitrification to >350 nM for homoacetogenesis. From Fig. 4 it can be observed that HCE reduction (0.6–0.9 nM) occurs at an overlapping H_2 threshold to Fe(III) reduction (0.1–0.8 nM) whereas LCE reduction overlaps with sulfate reduction and methanogenesis (Paul et al., 2016). Overlap of TEAP H_2 thresholds are commonly observed in experimental studies (e.g. Jakobsen and Postma, 1999; Aulenta et al., 2008; Paul et al., 2016) with lower levels than predicted from thermodynamic considerations (Heimann et al., 2009). This phenomenon has been attributed to kinetic effects arising from the relative efficiencies in H_2 producers and consumers in microbial consortia (Richardson, 2016).

2.2.3 Short chain fatty acids

Short-chain fatty acid (SCFAs) are labile DOC species such as butyrate, propionate and lactate produced as intermediates during primary DOC fermentation (Fig. 2) and are accompanied by an increase in pore water H^+ ion concentrations. SCFAs readily undergo secondary fermentation to produce electron donors (Giovannini et al., 2016). SCFA turnover is often the rate-limiting step in the anaerobic decomposition of complex DOM (Mani et al., 2016) and release of reducing equivalents for OHRB and other heterotrophs (Atashgahi et al., 2014). The most frequently reported SCFA in hyporheic zones is acetate which is both a terminal metabolite and intermediate of DOC fermentation (Fig. 2) (Baker et al., 1999; Baker and Vervier, 2004; Hlaváčová et al., 2005). It is an easily assimilated carbon source and possible direct electron donor for OHRB which may be independent of extracellular H_2 (Richardson, 2016). Under high pore water H_2 concentrations (>350 nM) acetate is also produced from other labile DOC compounds (i.e. methanol) or H_2/CO_2 by homoacetogens such as *Acetobacterium*, *Sporomusa*, *Spirochaeta* (Ziv-El et al., 2012).

Acetate has been widely shown to sustain respiration of HCEs as far as cDCE by facultative OHRB groups such as *Geobacter* and *Desulfuromonas* (Sharma and McCarty, 1996; Krumholz et al., 1996; Loffler et al., 2000; Wagner et al., 2012). For example, in contaminated aquifer media, Lee et al. (2007) found that whilst H_2 could sustain dechlorination of PCE as far as ethene, with uptake of acetate, dechlorination stalled at cDCE and proceeded at less than half the rate of H_2 alone. However, the role of acetate in OHR appears to be more complex. He et al. (2002) found that several organohalide-containing sediment microcosms amended with acetate alone were capable of sustaining PCE dechlorination to ethene. Their findings suggest a potential syntrophic partnership between cDCE and VC dechlorinators and acetate-oxidising bacteria (such as *Clostridium ultunense*) because of the low H_2 concentrations maintained by OHRB. Wei and Finneran (2013) also showed that acetate could sustain TCE, cDCE and VC dechlorination to ethene. Little difference in dechlorination rates were observed between amendments with 10 times more acetate. Similarly, higher production of acetate from solid organic polymeric materials used to stimulate cDCE in riverbed sediment microcosms did not lead to higher dechlorination rates as the excess organic loading was channelled to methanogenesis (Atashgahi et al., 2014). These results highlight the complex role acetate plays in anaerobic food webs with

sometimes contradictory effects observed in relation to OHR rates.

2.3 Interactions between OHR and alternative anaerobic TEAPs

Interspecies H_2 transfers between fermenters and anaerobic TEAPs (Fig. 3) including denitrification, metal reduction, sulfate reduction and methanogenesis (Fig. 4) may influence the rate and extent of OHR in anoxic zones (Aulenta et al., 2007). Toxic metabolites generated may also inhibit steps of the dechlorination process (Berggren et al., 2013). In this section, we review the current understanding of these competitive interactions between OHR steps and biogeochemical cycling in the hyporheic zone.

2.3.1 Nitrate reduction

Groundwater nitrate has become elevated over the last century as a result of the 6.4-fold increase in global inorganic fertiliser production between 1961 and 1999 (Peng et al., 2002). Heterotrophic denitrification producing nitrous oxide (N_2O) or dinitrogen (N_2) and dissimilatory nitrate reduction to ammonium (NH_4) occur in suboxic conditions (<125 μM O_2) with ambient H_2 levels (<0.1 nM) which are below the level at which OHR becomes favourable for HCEs (~0.6 nM) (Fig. 4). Nitrate respiration has only a slightly lower energy yield than that of oxygen with reaction timescales in the order of hours to days (Rivett et al., 2008a; Jahangir et al., 2012) and has been widely documented in hyporheic sediments (e.g. Ullah et al., 2014; Heppell et al., 2014). The interactions between OHR and nitrate respiration is apparently complex. Yu et al. (2014) have shown that nitrate stimulated OHR of pentachlorophenol at concentrations below 1 mM (likely by providing OHRB with a nitrogen source for growth) but became inhibitory at concentrations greater than 1 mM. This was supported by Chen et al. (2002) where 3 mM of nitrate inhibited hexachlorobenzene respiration under lactate-fermentation conditions in river sediments. Nelson et al. (2002) found PCE reduction inhibition from only 0.6 mM of nitrate and sulfate in a mixed culture where H_2 was continuously fed at non-limiting aqueous concentrations (0.4–0.8 mM). In that study, the metabolite N_2O was found to be an inhibitor of OHR at 13 μM. These results are consistent with capture of available electrons by denitrifiers and reduction of ambient H_2 levels below the minimum threshold necessary for OHRB as a key inhibition mechanism which is also in line with thermodynamic predictions and observed H_2 thresholds (Fig. 4).

255 **2.3.2 Iron(III) reduction**

256 Iron oxides and oxyhydroxides such as haematite (Fe_2O_3) and goethite ($FeO(OH)_3$) are abundant
257 primary and secondary minerals in streambed sediments which contain Fe(III) as a solid or colloidal
258 phase (Liu et al., 2014). Similarly, manganese oxide minerals such as pyrolusite (MnO_2) contain the
259 TEA Mn(IV) which behaves comparably to Fe(III) in redox processes (Ng et al., 2016). Some facultative
260 OHRB including *Desulfuromonas michiganensis* and *Geobacter lovleyi* (Sung et al., 2006) can also use
261 Fe(III) as a TEA. Dissimilatory Fe(III) reduction to Fe(II) has been observed at a similar H_2 threshold
262 range (0.1–0.8 nM) to HCE reduction (Fig. 4) and direct competition for electron equivalents is therefore
263 possible over reaction timescales measured months. Inhibition of TCE reduction as a result of Fe(III)
264 was demonstrated in microcosm studies prepared from dolomite aquifer materials (Yager et al., 1997).
265 Dupont et al. (2003) observed general inhibition of TCE reduction due to a large pool of bioavailable
266 Fe(III) minerals in microcosms prepared from contaminated aquifer sediment. In contrast, Wei and
267 Finneran (2011) demonstrated simultaneous reduction of TCE to ethene and Fe(III) to Fe (II) in
268 microcosms dominated by *D. mccartyi* and *Geobacter* with an excess of electron donor. Fe(III) was
269 observed to facilitate OHR by maintaining the ambient H_2 concentration at a level favourable for the
270 OHRB. Using the 'KB-1' organohalide-respiring enrichment culture (Duhamel et al., 2002), Paul et al.
271 (2013) showed that pH and iron mineral structure play an important role in inhibition of OHR in assays
272 of 14 different synthetic Fe(III) minerals using an excess of formate as an electron donor. High-surface
273 area, poorly crystalline minerals (such as ferrihydrite) have a greater Fe(III) fraction which is
274 bioavailable for electron transfer than highly crystalline minerals such as haematite and goethite. These
275 studies suggest the inhibition of OHR by Fe(III) in hyporheic sediments is complex and will be strongly
276 linked to pH, specific bioavailable iron mineral composition, surface area and sediment particle size
277 rather than total sediment Fe(III) content (Paul et al., 2013; 2016).

278 **2.3.3 Sulfate reduction**

279 Sulfate is a major oxyanion in groundwater derived from chemical denudation of sedimentary
280 rocks, oxidation of sulfide minerals and anthropogenic point sources. Dissimilatory sulfate reduction to
281 sulfide occurs at similar observed H_2 thresholds (1–15 nM) to HCE and LCE respiration (Fig. 4). The
282 presence of sulfate has been widely implicated where incomplete dechlorination leads to the

accumulation of LCEs (e.g. Bagley and Gossett, 1990; Pavlostathis and Zhuang, 1993; Lorah et al., 2007) although laboratory studies of interactions between sulfate reduction and OHR are inconclusive. For example, sulfate reduction was reported to affect rates of VC respiration and to a lesser extent cDCE respiration (Boopathy and Peters, 2001; Aulenta et al., 2008; Pantazidou et al., 2012). Hoelen and Reinhard (2004) observed respiration of TCE at sulfate concentrations of 1–2.6 mM in sediment microcosm containing CEs and alkyl benzenes. TCE reduction was found to inhibit sulfate reduction under an ambient H_2 concentration of 0.7 nM. Sulfate reduction at higher H_2 levels (2.5 nM) was observed to compete with reduction of cDCE and VC which was sustained at a H_2 concentration of 1.6 nM. With constant H_2 concentrations (2–4 nM) sustained by lactate fermentation, Berggren et al. (2013) found that the addition of sulfate affected the cDCE to VC respiration step the greatest (67%) in comparison to VC to ethene (25%) and TCE to cDCE (8%). This work showed that sulfate addition could produce a shift in the community structure of *D. mccartyi* leading to a reduction in OHR rates. In contrast, an absence of any inhibitory effect under non-limiting electron donor conditions were shown (e.g. Hoelen et al., 2006; Aulenta et al., 2007) and even sulfate addition was reported to strongly enhance TCE respiration (Harkness et al., 2012). This may be a result of syntrophic partnership between sulfate reducers and OHRB through provision of essential nutrients such as corrinoids (Men et al., 2012, Sutton et al., 2015; Lu et al., 2017 Atashgahi et al., 2017a). A recent study on isolates, constructed consortia and enrichments containing *D. mccartyi* showed that rather than sulfate, sulfide inhibited the growth of *D. mccartyi* and its syntrophic partner, *Syntrophomonas wolfei* (Mao et al., 2017). Interestingly, in a co-culture of *D. mccartyi* and sulfate-reducing *Desulfovibrio vulgaris* Hildenborough, a high sulfate concentration (5 mM) was not inhibitory to OHR under electron donor (lactate) limitation likely due to strong electron scavenging capacity of *D. mccartyi*. Moreover, at low sulfate levels (2 mM), sulfate reduction was not inhibitory even under excess of electron donor (Mao et al., 2017).

2.3.4 Methanogensis

Methanogenesis represents the final phase of anaerobic DOM metabolism (Figs 2 and 4) with methane production timescales in riverbed sediments reported in the order of 200 days (Sela-Adler et al., 2017). Its importance as a metabolic process in hyporheic zones is becoming increasingly recognised (e.g. Sanders et al., 2007; Shelley et al., 2014; Brablcová et al., 2015). Methanogens are dependent on

the same key substrates and electron donors as OHRB including acetate (via acetoclastic methanogenesis) and H_2 (through hydrogenotrophic reduction of CO_2). The effects of acetoclastic methanogenesis on OHRB is less well understood than hydrogenotrophic methanogenesis. Heimann et al. (2006) suggested that acetoclastic methanogenesis may enhance VC dechlorination by providing additional H_2 during acetate cleavage. The observed H_2 thresholds for hydrogenotrophic methanogenesis (5–100 nM) are considerably greater than OHR (0.1–2.5 nM) (Paul et al., 2016) and OHRB have been shown to out-compete hydrogenotrophic methanogens for reducing equivalents at low H_2 concentrations (Ballapragada et al., 1997; Yang and McCarty, 1998; Azizian et al., 2010). CEs on the other hand have been shown to have direct inhibitory effect on methanogenesis through enzyme inactivation although the effect is less pronounced than for other organohalides such as chlorinated methanes (Chan and Radom, 2011). Yu and Smith (2000) found that 137 μM of TCE could inhibit methanogenesis but no effect was observed from PCE at 87 μM. In enrichment cultures containing fermenters, *D. mccartyi* strain 195, homoacetogens and methanogens, Men et al. (2013) found that 22 μM of TCE caused inhibition of hydrogenotrophic methanogenesis with an increase of electron flow to OHR by an average of 7% under non-limiting H_2 concentrations (7–12 nM). Their results suggested that TCE could inhibit homoacetogenesis at H_2 levels well above the optimal range for OHRB. That study showed that non-methanogenic cultures generated significantly more ethene faster than methanogenic cultures and suggested that fermenters (*Clostridium* spp.) may also supply essential nutrients (corrinoids) in addition to H_2.

2.3.5 Co-mingled organohalides

An important consideration in the anaerobic transformation potential of hyporheic zones for CEs is the presence of other organohalides in co-mingled groundwater plumes. The chlorinated ethane 1,1,1-trichloroethane (1,1,1-TCA) introduced as an alternative to TCE and the chlorinated methane, chloroform, (TCM) are frequent co-contaminants (Scheutz et al., 2011; Simsir et al., 2017). TCM is also produced from natural processes in soils at low concentrations (<10 μM) (Laturnas et al., 2002). Both 1,1,1-TCA and TCM have been implicated in the accumulation of LCEs and VC in particular (Duhamel et al 2002; Chung and Rittmann, 2008; Chan et al., 2011). TCM has also shown to inhibit dechlorination of cDCE by *D. mccartyi*. (Maymo-Gatell et al., 2001). Conversely, Grostern et al. (2009) showed that

VC and cDCE to lesser extent can cause inhibition in the respiration of chlorinated ethanes (CAs) (1,1,1-trichloroethane and 1,1-dischloroethane) Mayer-Blackwell et al. (2016) found that prolonged exposure to 1,2-dichloroethane (DCA) in a VC-respiring culture caused selective changes in *D. mccartyi* community structure and reduced VC-respiration capacity. Strong inhibition of DCA respiration was observed by cDCE. At field scale, Simsir et al. (2017) observed no inhibitory effect on the CE dechlorination capacity of hyporheic sediments due to the spatial segregation of CE and CA dechlorinators (demarcated by expression of the *cfrA* gene associated with CA respiration) along discharging groundwater flow paths. CEs themselves may also competitively inhibit steps of the OHR sequence (Chambon et al., 2013). In a kinetic study using two mixed anaerobic cultures, Yu et al. (2005) found that HCEs generally inhibited the respiration of LCEs whilst the LCEs weakly inhibited the dechlorination of the HCEs. These studies highlight the complex inter-relationship between different organohalide respiration steps and their metabolites.

2.4 Development and implications of anoxic-oxic interfaces

The higher halogen substitution of HCEs produces electrophilicity with resistance to electrophilic attack by oxygenase enzymes of aerobic bacteria. Thus, oxidation of the carbon backbone of the ethene molecule is energetically unfavourable (Vogel et al., 1987). Schmidt et al. (2014) recently reported aerobic TCE oxidation as a sole carbon source which may be evidence of a novel metabolic process not witnessed before. Nonetheless, susceptibility to the reductive pathway decreases proportionately with the ratio of chlorine to carbon substituents. As such, LCEs may be amenable to transformation via aerobic mineralisation pathways during hyporheic exchange flows (Atashgahi et al., 2013). From a natural attenuation perspective, mineralisation reactions are attractive in that no stable toxic intermediates generated (Tiehm and Schmidt, 2011).

2.4.1 Hyporheic oxygen gradients and mixing zones

A unique feature of hyporheic zones is the establishment of oxic domains located where river water infiltrates bringing dissolved O_2 into riverbed pore water at saturation concentrations (Knapp et al., 2015). A common scenario illustrating development of a shallow oxic zone within a predominantly anoxic groundwater regime is depicted in Fig. 5 based on the conceptual framework of Figs 1 and 2. In

366 this situation, river water advection is induced by bed topography in a process known as hyporheic
367 exchange flow where water currents infiltrate on the upstream side of a topographic feature
368 (downwelling zone) and return back to surface water a short distance downstream along with
369 groundwater discharge (upwelling zone) (Harvey and Bencala, 1993; Gomez-Velez et al., 2014; Trauth
370 et al., 2015). These bi-directional hyporheic flow cells (HFCs) will develop at various scales around bed
371 and channel topographic features such as gravel bars, riffles, weirs, debris dams and meanders (Krause
372 et al., 2014; Boano et al., 2014; Fox et al., 2014).

373 A thin mixing zone (Fig. 5); governed by dispersive processes is thought to develop along the
374 boundary between HFCs and the surrounding groundwater-dominated pore water regime which is
375 characterised by unidirectional vertical and lateral flow paths (Zarnetske et al., 2012; Briggs et al., 2013;
376 Binley et al., 2013; Boano et al., 2014). Numerical simulations of conservative tracer transport through
377 hydrologically gaining hyporheic zones (Hester et al., 2013) have suggested that the thickness of this
378 mixing zone is greatest with homogeneous high K sediment (e.g. well-sorted sand or gravel) and reduced
379 groundwater discharge (Fig. 5). Conversely, in zones of elevated groundwater discharge, low stream
380 velocity and smooth bed topography the mixing zone may be reduced or absent entirely (Trauth et al.,
381 2015). During high river flows, HFCs and associated mixing zones may transiently penetrate into deeper
382 sediment layers which is accompanied by a temporary surface water invasion of the groundwater regime
383 at depth (e.g. Cuthbert et al., 2010; Hamonts et al., 2012; Byrne et al., 2013; Freitas et al., 2015). These
384 transient flow events may be particularly acute for urban rivers where peak flows are accentuated by
385 impervious catchment areas and channel canalisation (Meyer et al., 2005).

386 Advection of river water solutes including O_2 and DOM into bed sediments induces zones of
387 aerobic respiration (Fig. 5) where the reaction timescale is often rapid with zero-order rates reported
388 from 9 and 75 µM/h in a gravel bar (Vieweg et al., 2016). Where mixing occurs, an anoxic-oxic interface
389 will develop which shifts dynamically in response to the balance of surface water downwelling and
390 groundwater discharge pressures. Approximately 0.25–0.33 mM of DOC is required to deoxygenate
391 downwelling river water and other reductants from the anoxic zone (Fig. 4) such as Fe(II) and reduced
392 sulfur species may also consume O_2. Hence, conditions for a spatially fluctuating 'reactive fringe'

(Trauth et al., 2014) where complementary aerobic co-metabolic or growth-coupled assimilation of cDCE and VC may be favoured. As a result, hyporheic zones can offer a spatially variable secondary aerobic 'treatment' zone facilitating complete mineralisation of LCE metabolites (Atashgahi et al., 2013; 2017a).

2.4.2 cDCE mineralisation

Although cDCE is amenable to aerobic biotransformation, cDCE oxidation is not widely reported. Bradley and Chapelle (1998a) were among the first to examine the potential for aerobic cDCE mineralisation in microbial communities indigenous to riverbeds. Their study demonstrated biological aerobic mineralisation of [^{14}C]-DCE (4:1 *cis*-to-*trans* isomers) to CO_2 in microcosms with recovery of [^{14}C]-CO_2 ranging from 17–100% after just eight days. However, this study used natural sediment media potentially containing a range of other substrates where co-metabolic processes could not be ruled out (Bradley and Chapelle, 2000). Other work has shown aerobic cDCE mineralisation to proceed much more slowly in aquifer media e.g. Klier et al. (1998) where just 3−10% mineralisation was achieved after 180 days incubation. Moreover, Abe et al. (2009) found no evidence of cDCE removal in aerobic riverbed microcosms incubated over 1.5 years. Such patchy metabolic cDCE aerobic degradation is illustrated by the fact that only a single isolate, *Polaromonas* sp. JS666 has unequivocally shown to grow by cDCE assimilation as the sole carbon and energy source (Coleman et al., 2002). With the advent of compound-specific stable isotope analysis (CSIA), kinetic isotope fractionation of carbon (δ^{13}C-cDCE) has provided an additional line of evidence that cDCE mineralisation may be a growth-linked assimilatory process. Reported δ^{13}C enrichment factors for aerobic uptake of cDCE range from −7.1‰ to −22.4‰ for both mixed and pure cultures (Tiehm et al., 2008; Abe et al., 2009; Schmidt et al., 2010). Biomass yields from cDCE uptake are reported to range from 6.1 to 12.5 g/M cDCE (Coleman et al., 2002; Schmidt et al., 2010).

2.4.3 VC mineralisation

VC mineralisation is the most thermodynamically attractive CE oxidation process due to the presence of only one chlorine substituent. Reaction timescales tend to be relatively rapid as a result. In a radiolabelled microcosm study prepared from riverbed sediments (Bradley and Chapelle, 1998a), it

420 was shown that greater than 90% of VC was consumed after 12 days over a concentration range of 0.2
421 – 57 μM with uptake rates most adequately described by Michaelis-Menten kinetics. Bacteria capable
422 of aerobic VC oxidation as a sole carbon and energy source belong to a range of genera associated with
423 aerobic ethene assimilation (Mattes et al., 2010; Atashgahi et al., 2017a). Aerobic degradation of VC
424 and ethene are initiated by an alkene monooxygenase (EtnABCD) and an epoxyalkane-coenzyme
425 enzyme (EtnE) (Mattes et al., 2010). Various isolates have been identified including *Mycobacterium*
426 (Hartmans et al., 1985; Hartmans and DeBont, 1992; Fullerton et al., 2014; Le and Coleman, 2011),
427 *Pseudomonas* (Verce et al., 2000; 2001; Atashgahi et al., 2017a), *Ochrobactrum* (Danko et al., 2004,
428 Atashgahi et al., 2017a), *Nocardioides* (Coleman et al., 2002) and a *Ralstonia* (Elango et al., 2006).
429 Besides these classical VC-assimilators, stable isotope probing coupled to high-throughput 16S rRNA
430 gene sequencing and quantitative polymerase chain reaction (qPCR) extended the potential range of VC
431 assimilators to *Sediminibacterium*, *Aquabacterium*, *Variovorax*, *Brevundimonas*, *Tissierella*, and
432 *Rhodoferax*. (Paes et al., 2015; Wilson et al., 2016). Gossett (2010) found that biological VC respiration
433 could be sustained by *Mycobacterium* at extremely low (microaerophillic) extracellular O_2
434 concentrations (e.g. 0.3–0.6 μM). This finding raises the important question as to whether anoxic
435 conditions classically defined by O_2 concentrations less than 3 μM (Chapelle and McMahon, 2006) are
436 in fact still capable of supporting aerobic metabolism. Microaerophilic VC oxidation may also play a
437 role in the apparent 'stalling' of the dechlorination sequence at cDCE. A lack of VC detection may in
438 fact reflect scenarios where VC mineralisation rates equal or exceed the production rate under hypoxic
439 conditions (Bradley and Chapelle, 2011). In a recent microcosm study by Fullerton et al. (2014) subject
440 to inadvertent O_2 contamination, VC disappearance was observed without ethene formation. A strictly
441 aerobic *Mycobacterium* was identified in high numbers in the groundwater microcosm which was
442 inadvertently exposed to O_2. Atashgahi et al. (2013, 2017a) used 16S rRNA of *D. mccartyi* and genes
443 encoding for reductive dehalogenase enzymes (*vcrA* and *bvcA*) and the genes *etnC* and *etnE* involved in
444 aerobic mineralisation of VC and ethene to track the fate of VC in microcosms prepared from riverbed
445 sediments obtained from anoxic-oxic interface. Using a combination of chemical analysis and qPCR,
446 the authors demonstrated co-occurrence and co-activity of aerobic VC degraders and anaerobic *D.*
447 *mccartyi* in hyporheic sediments of the eutrophic Zenne River in urban Belgium (Atashgahi et al.,

448 2017a).

449 **2.4.4 Aerobic co-metabolism**

450 CEs can be transformed under aerobic conditions by co-metabolic reactions initiated by common
451 enzymes produced by a wide range of aerobes (Arp, 1995). No known benefit is gained through
452 acquisition of metabolic energy or biomass production (Horvath 1972; Wacket, 1988; Semprini et al.,
453 1994). Co-metabolism is a widespread process by microbes containing non-specific monooxygenase or
454 dioxygenase enzymes which catalyze the initial step in oxidation of a growth-supporting substrate in the
455 presence of O_2 (Suttinun et al., 2013). A lack of enzyme specificity leads to competition between CEs
456 and growth-supporting substrates for active sites of oxygenases leading to incorporation of O_2 into the
457 chloroethene molecule via reactive epoxide formation (Mattes et al., 2010). TCE, cDCE and VC are all
458 amenable to co-metabolic aerobic oxidation by the action of oxygenases. PCE was originally thought to
459 be recalcitrant to aerobic oxidation under environmental conditions, however it is shown to be
460 degradable by the enzyme toluene-*o*-xylene monooxygenase (Ryoo et al., 2000; Shim et al., 2001).

461 In hyporheic sediments, methane and ammonium are often the most abundant potential substrates
462 for co-metabolism produced from the in-situ anaerobic decomposition of DOM (Figs 2 and 5) (Donn
463 and Barron, 2013; Atashgahi et al., 2013; Brablcová et al., 2015; Simsir et al., 2017). Extensive
464 hyporheic methanotrophy has been documented in association with fine-grained sediments under
465 vegetation stands in streams (Sanders et al., 2007) and in well-oxygenated coarse-grained sediments
466 (Trimmer et al., 2010). The enzyme methane monooxygenase is produced by the methanotroph
467 *Methylosinus trichosporium* and has been shown to oxidise TCE, cDCE, VC and ethene (Oldenhuis et
468 al., 1991; Forrester et al., 2005; Findlay et al., 2016). Conrad et al. (2010) observed evidence of co-
469 metabolic TCE oxidation at field-scale in a contaminated aquifer with an increase in *M. trichosporium*
470 abundance accompanied by a decline in TCE and dissolved methane concentrations. A co-metabolic
471 process was verified in a supporting microcosm study prepared from aquifer media and isotopically-
472 labelled TCE (^{13}C-TCE). Simsir et al. (2017) presented evidence of possible hyporheic zone co-
473 metabolism with declines in cDCE and VC associated with strong vertical methane gradients (Fig. 6)
474 although no O_2 data are presented for comparison. Their study also documented the presence of

475 methanotrophs (*Methylococcaceae* spp.) coincident with the change in methane concentrations in the
476 sediment sequence. Nitrifying bacteria which oxidise ammonium produced from DOM metabolism (Fig.
477 2) such as *Nitrosomonas europaea* can also inadvertently oxidise TCE and LCEs (Arciero et al., 1989;
478 Vannelli et al., 1990; Rasche et al., 1991; Kocamemi and Cecen, 2005). Nitrification is well documented
479 in association with hyporheic flow cells (Jones, 1995; Briggs et al., 2013). Kocamemi and Cecen (2005)
480 found that ammonium and TCE compete for the same active sites of the enzyme ammonia
481 monooxygenase. In a mixed culture study containing *Nitrosomonas europaea,* Kocamemi and Cecen
482 (2010) found that the transformation yield for TCE was strongly dependent on initial ammonium and
483 TCE concentrations, with a minimum initial level of 3 μM of ammonium required to transform the
484 maximum initial TCE concentration of 7 μM. We are not aware of any studies which have considered
485 hyporheic nitrification as a natural attenuation process for CEs under field conditions.

486 **2.4.5 Interaction between aerobic and anaerobic VC transformation pathways**

487 Ethene-assimilating bacteria (ethenotrophs) can oxidise ethene as the sole carbon and energy
488 source and simultaneously transform VC co-metabolically whereas VC-assimilating bacteria can use
489 VC as the sole carbon and energy source (Mattes et al., 2010). Therefore, when anoxic groundwater
490 containing VC and ethene migrates through the mixing zones around HFCs, there is a potential for
491 assimilation of both substrates by ethenotrophs and VC-assimilators and also co-metabolic VC
492 degradation by ethenotrophs growing on ethene (Atashgahi et al., 2017a). Such synergetic interactions
493 can be further enhanced by methanotrophs that can oxidize both ethene and VC. In line with this, a
494 recent study using groundwater microcosms showed that when methane, ethene and VC were added to
495 microcosms, the rate of VC removal was faster than with either methane or ethene alone, consistent with
496 the idea that methanotrophs stimulate ethenotrophic removal of VC (Findlay et al., 2016). Moreover,
497 recent studies have shown that reductive dechlorination can impact aerobic VC degradation pathways
498 in hyporheic zones. Microcosms prepared from fine-grained, SOM-rich sediments with high reductive
499 dechlorination capacity did not have the potential for metabolic aerobic VC oxidation (Atashgahi et al.,
500 2013, 2017a). Under atmospheric O_2 conditions, *D. mccartyi* was protected from O_2 toxicity by the
501 sediment structure and grew by reductive dechlorination of VC. No ethene accumulation was noted
502 indicating the activity of ethenotrophs (Atashgahi et al., 2013, 2017a) which can, in turn, co-

503 metabolically oxidise VC (Findlay et al., 2016). In contrast, metabolic aerobic VC activity was observed
504 from microcosms prepared from sediments with low SOM, coarse grain size and low reductive
505 dechlorination potential. The study showed that local sediment geochemistry and reductive
506 dechlorination highly impact metabolic versus co-metabolic aerobic VC degradation pathway. Where
507 low reductive potential was noted, ethenotrophs exposed to continuous VC flow in oxic sediment layers
508 might adapt to metabolic aerobic VC degradation (Atashgahi et al., 2017a). These findings are consistent
509 with upon extended exposure to VC, ethenotrophic strains of *Mycobacterium* (Jin and Mattes, 2008) and
510 *Pseudomonas* (Verce et al., 2001) transit from co-metabolic to growth-linked VC mineralisation.

511 ## 3 Field-scale conceptualisation challenges and potential solutions

512 ### 3.1 Spatial variability of potential transformation zones

513 #### 3.1.1 OHRB occurrence in riverbed sediments

514 qPCR approaches targeting 16S rRNA genes and reductive dehalogenation catabolic genes (*rdhA*)
515 (Lu et al., 2015) have been used to track the presence and activity of OHRB in hyporheic zones
516 (Vandermeeren et al., 2014). These biomarkers have revealed a close association with OHRB, SOM
517 content and grain-size distribution in organohalide-impacted hyporheic sediments (Atashgahi et al.,
518 2013; Kranzioch et al., 2013; Hamonts et al., 2014; Atashgahi et al., 2015). In a survey of OHRB in
519 relation to hexachlorobenzene (HCB) fate in 15 riverbed sediment locations across four European
520 catchments, Taş et al., (2011) detected *D. mccartyi* 16S rRNA genes at 80% of sites though their counts
521 did not surpass 0.1% of total bacterial 16S rRNA gene copies. HCB half-lives ranged from a few days
522 to up to one month. A relatively weak correlation was observed between decay rate and number of *D.*
523 *mccartyi* suggesting additional OHR activity from other OHRB. Atashgahi et al. (2013) used 16S rRNA
524 of *D. mccartyi* and genes encoding for VC reductive dehalogenase enzymes (*vcrA* and *bvcA*) to track
525 dominant VC biotransformation processes in microcosms prepared from hyporheic sediments. *D.*
526 *mccartyi* had a dominant role on VC removal in microcosms prepared from coarse-grained bed
527 sediments with an abundance of SOM. A subsequent in situ study at the same site showed a reduced VC
528 respiration potential due to construction of a wastewater treatment plant upstream of the study area that
529 resulted in a reduction of organic matter loading to the riverbed sediments (Atashgahi et al., 2015).

Similarly, PCR detection of *D. mccartyi* was reported to be closely linked with SOM content and sediment particle size (Abe et al., 2009). This work showed that *D. mccartyi* presence in the sediment profile was spatially correlated with SOM where it exceeded 2% (g/g) with stronger signals occurring at greater depth. A recent study by Simsir et al. (2017) investigated CEs discharging to a creek in Tennessee from organohalide-contaminated fractured bedrock (Table 1). Over a 300 m river section, 16S rRNA genes of *D. mccartyi* and *Dehalobacter* were found to be more abundant in deeper sediment layers (50 cm) coincident with higher concentrations of cDCE and VC. Their study revealed the presence of multiple strains of *D. mccartyi* occurring together and expressing functional genes involved in respiration of CE (e.g. *tceA*, *bvcA* and *vcrA)* and chlorinated ethane/methane (*dcpA*).

3.1.2 Plume-scale discharge and transformation controls

Groundwater plume discharge and transformation patterns are controlled by the spatial distribution and continuity of sediment domains with distinct hydraulic properties along river corridors (Fleckenstein et al., 2006; Wondzell, 2011). The available field investigations (Table 1) have shown that low-K sediments (e.g. clay and silt) are the most important local controls on contaminant discharge in heterogeneous sediment sequences. For example, at the Pine River PCE plume site in Ontario (Conant et al., 2004; Abe et al., 2009) and for a TCE plume discharging to the River Tern in the UK (Weatherill et al., 2014), the lateral and longitudinal continuity of semi-confining silty deposits were shown to control the location and magnitude of plume discharge (Table 1, Fig. 6). Where these low-K sediments also contain SOM, conditions for enhanced biotransformation may also occur where residence times are greatly extended due to hydrophobic portioning to the organic carbon present. This is demonstrated by Conant et al. (2004) and Abe et al. (2008) for the Pine River site with extensive in-situ transformation of PCE or TCE to cDCE (Fig. 6) reported. The importance of low-K layers in contaminant transformation has been illustrated in a modelling study by Gomez-Velez et al. (2014). Their work has shown that the interfaces of sediments with large K contrasts can sequester upwelling groundwater by creating stagnation zones which facilitate mixing of waters with different residence times. Hyporheic exchange patterns arising from riverbed topography have also been shown to influence patterns of in-situ transformation of discharging groundwater plumes. With the benefit of chloride as a conservative surface water tracer, Freitas et al. (2015) observed TCE transformation associated with coarse grained

558 sediment along a riffle sequence of the River Tame (Birmingham, UK) where river water infiltration
559 carrying DOC was inferred from chloride profiles. In one location (Fig. 6) up to 80% TCE conversion
560 to ethene was reported. In-situ dechlorination was also shown to be largely absent along the investigation
561 corridor where riverbed topography was subdued.

562 The presence of preferential pathways with short residence times (such as springs) afford little
563 opportunity for in-situ natural attenuation (e.g. Fryar et al., 2000; LaSage et al., 2008; Rønde et al.,
564 2017). This mode of contaminant discharge arises where discontinuities occur in low-permeability
565 alluvial architecture that act as high-flux 'geological windows' (Conant et al., 2004; Weatherill et al.,
566 2014). For example, through temperature mapping, Conant (2004) found that nearly a quarter of the
567 baseflow accretion along a reach of the Pine River in Angus occurred from just 7% of the riverbed area.
568 The available case studies (Table 1) highlight the patchy nature of natural attenuation zones where the
569 mass fluxes to surface water are dominated by small areas through which most groundwater baseflow
570 discharge is concentrated.

571 **3.1.3 Pore-scale mass transport and processing**

572 Microbial metabolic activity and diversity in riverbeds has been reported to be concentrated in
573 the uppermost 50–60 cm of hyporheic sediment sequences (Franken et al., 2001; Freixia et al., 2016).
574 Heterotrophic microbes (including OHRB) are predominantly found attached to sediment surfaces in
575 epilithic biofilms (Davey and O'Toole, 2000). Hyporheic biofilms comprise diverse assemblages of
576 fungi, algae and microbial consortia enveloped by a matrix of extracellular polymeric substances (EPS)
577 through which diffusive transport of solutes predominates (Storey et al., 1999; Battin et al., 2016).
578 Biofilm structures have been shown to retain and process complex DOM in sediments (Fischer et al.,
579 2005; Bengtsson et al., 2014) and may be important sites of SCFA fermentation (Rulík and Hereka,
580 1998; Rulík et al., 2000). Biofilm accumulation in interstitial spaces is known to decrease the bulk K
581 and effective porosity of sediments in downwelling zones, thereby reducing hydrodynamic exchange
582 with the overlying water column (Battin et al., 1997; 2003; 2008; Mermillod-Blondin et al., 2005) and
583 inducing redox gradients (Boano et al., 2014). Biofilm development may be facilitated in downwelling
584 streambed zones during the clogging of coarse sediment pore spaces (colmation) by non-settlable POM

originating from surface water sources (Navel et al., 2012).

The convolution of flow paths through heterogeneous biofilm-enveloped sediments produces a scale dependence in chemical reaction rates where microbial processes are superimposed on larger-scale advective solute fluxes that deliver reactants (Sobczak and Findlay, 2002; Findlay et al., 2003; Nogaro et al., 2013). Mendoza-Lera et al. (2017) propose a conceptual framework unifying hyporheic flow and biogeochemical transformation capacity in riverbeds which is applicable for both anaerobic and aerobic biotransformation of CEs. They propose that biogeochemical processing is controlled by the mass transfer of key reactants (TEAs, fermentable DOM and nutrients) and the sediment surface area available for biofilm colonisation. Mass transfer is characterised in three stages, the slowest of which will be the rate-limiting step for biotransformation: (1) transfer from bulk groundwater or surface water to the hyporheic environment (2) transfer from sediment pore water into microbial biofilms and (3) membrane transfer from the extracellular biofilm matrix into individual cells. The sediment particle size controls the surface area for colonisation which is inversely proportional to K. High K sediments (such as gravel bars) exhibit high mass transfer rates but low processing capacities. Conversely, low K sediments (e.g. silts and clays) have very high areas for colonisation due to the huge surface area to sediment volume ratio present but mass transport is slow and diffusion-limited. Their model assumes that solute uptake rates follow Michaelis-Menten kinetics where microbial activity increases proportionally with the mass transfer rate until a saturation point is reached (Ribot et al., 2013). This framework supports field observations where enhanced dechlorination activity and OHRB are reported in sediment domains where diffusive transport is locally dominant (Conant et al., 2004; Abe et al., 2009; Damgaard et al., 2013; Atashgahi et al., 2015; 2017a). Biofilm colonisation is also influenced by changes in pore water temperature, pH and light exposure as well as sediment surface roughness (Gette-Bouvarot et al., 2015; Voisin et al., 2016).

Delivery of CEs into reactive diffusion-dominated pore water systems will be dependent on the presence, connectivity and residence time of macropore flow paths which facilitates advective transfer from bulk upwelling groundwater (e.g. Bohlke et al., 2007; Chambon et al., 2010; Menichino and Hester, 2015). Heterogeneity in grain size distribution, particle packing and sphericity can induce locally anoxic

or hypoxic microzones where mass transfer rates from bulk water to biofilms vary at the scale of sediment pores (Briggs et al., 2013; 2014). Anoxic microzones have been widely implicated where mixed TEAPs and fermentation reactions appear to occur simultaneously (e.g. Storey et al., 1999; Baker et al., 2000; Mermillod-Blondin et al., 2005) and may explain observed co-activity of aerobes and anaerobes (e.g. Atashgahi et al., 2017a). Using two-dimensional dual-domain pore network models of advective-diffusive transport, Briggs et al. (2015) showed that pore-scale heterogeneity (variation in pore throat size) leads to zones of increased and decreased solute mobility in hyporheic in hyporheic sediments. In the less mobile domain (which is responsible for observed tracer breakthrough tailing), anoxia develops where O_2 consumption exceeds the re-supply rate. These microzones may be cumulatively important in determining the overall transformation capacity of hyporheic sediments. For example, LCEs produced anaerobically in the low-mobility domain are mineralised in the more mobile aerobic domain. This is particularly important in the case of VC which can require only trace oxygen levels to sustain aerobic uptake (Gossett, 2010; Fullerton et al., 2014).

3.2 Multi-scale in-situ characterisation technologies

3.2.1 Evaluating hydrological connectivity

The natural flow regime heterogeneity of most plume discharge zones makes the design and implementation of effective in-situ monitoring programs non-trivial (Kalbus et al., 2006; Rivett et al., 2008b; Roy and Bickerton, 2010; Burk and Cook, 2015). Heterogeneous sediment sequences present a common challenge for the development of conceptual models of plume fate (Ellis and Rivett, 2007). Direct sediment core sampling can provide intact samples in cohesive sequences but is impractical where granular deposits occur. Freeze-coring methods have been applied to characterise fluvial sediment sequences with mixed grain size distributions (Freitas et al., 2015). However, this extractive technique necessitates disruption of sediment microstructure and associated transport pathways (Descloux et al., 2010). Non-invasive hydrogeophysical 'imaging' technologies have emerged which offer promising insights into the in-situ spatial variability of mass transport pathways at <1 m to >10 m scales. For example, Mermillod-Blondin et al. (2014) used ground-penetrating radar (GPR) to map biologically active domains within a gravel bar sequence of the River Rhone in France. Electrical resistivity imaging technology has been used to image flow-controlling sedimentary structures and electrically conductive

solute plume migration at reach-scale (Nyquist et al., 2008; González-Pinzón et al., 2015). Recently, Briggs et al. (2014) applied geoelectrical hysteresis techniques to characterise pore-scale rate-limiting mass transport through dual domain porous media (mobile and less mobile porosity fractions).

Temperature mapping using contact probes or continuous optical fibres and has been used to evaluate patchy sub-metre scale connectivity between groundwater and surface water in plan-view when a seasonal thermal gradient is present (Conant, 2004; Tristram et al., 2014; Rosenberry et al., 2016). Groundwater baseflow fluxes through riverbeds have been modelled using one dimensional advective-diffusive heat flow as a surrogate for Darcian flow in grids of riverbed temperature profiles (Schmidt et al., 2006; 2007) where upwelling flow predominates. Both upwelling and downwelling fluxes have more recently been obtained from vertical profiles of riverbed temperature time series (e.g. Anibas et al., 2011; 2016; Munz et al., 2016). Heat pulse injections have been used to understand three-dimensional water fluxes through shallow sandy hyporheic sediments at centimetre scales (Angermann et al., 2012). Recently, point-velocity probing (PVP) has been used to map hydrological connectivity with a comparable resolution to temperature mapping (Rønde et al., 2017). Overall, hydrological connectivity will be highly site-specific and the most useful results will be obtained where multiple techniques are employed with overlapping nested scales (e.g. Milosevic et al., 2012).

3.2.2 Resolving in-situ biogeochemical gradients

Delineation of in-situ vertical chemical gradients has been accomplished using depth-discrete profiling in riverbeds (Fig. 6) over vertical length scales of 0.1 to 3 m (Conant et al., 2004; Rivett et al., 2008b; Krause et al., 2013; Heppel et al., 2014). Multi-port monitoring wells have achieved finer vertical sampling resolution (<0.1 m) in contaminated aquifers (e.g. Jobelius et al., 2011). However, technical challenges and cost implications are often likely to prohibit monitoring installations in riverbeds which require a drilling rig. Instead, hand-portable lightweight installations utilising drive-point and direct-push methods usually offer the most cost-effective solutions (Rivett et al., 2008b; Roy and Bickerton, 2010). CE fate in hyporheic systems has been investigated using the 'waterloo profiler' (Pitkin, et al., 1999; Conant et al., 2004) and other pore water samplers (e.g. Hamonts et al., 2012), multi-level sampler bundles (Conant et al., 2004), nested piezometers (Lorah and Olsen, 1999) and drive-point mini-

667 piezometers (Conant et al., 2004; Ellis and Rivett, 2007; Roche et al., 2008). Rivett et al. (2008b) and
668 Typical drive-point methods utilise a temporary casing to protect screens and sampling inlets during
669 installation. Collapse of adjacent sediments is relied upon to provide sufficient sealing action to prevent
670 any preferential flow along this 'short-circuit' pathway. This limitation is overcome with direct-push
671 methods such as that described by Roy and Bickerton (2010). They developed a miniaturised waterloo
672 profiler optimised for rapid acquisition of riverbed sediment pore water using a portable hammer drill.
673 From Fig. 6 and Table 1, it can be seen that the selection of appropriate vertical monitoring scales is
674 site-specific and must be informed by an initial conceptual understanding larger scale water fluxes.
675 Recent field experience suggests vertical resolutions of 0.1 – 0.2 m may be sufficient to capture bulk
676 gradients in pore water chemistry (Fig. 6).

677 A potential monitoring gap exists at μm–mm scales below the sediment-water interface where
678 preservation of natural stratification in pore water chemistry is impossible with extractive sampling
679 techniques. Transformation boundary zones at thin fine-grained sediment strata and critical mixing
680 zones may be overlooked by sampling at coarser resolutions (Hester et al., 2017). In-situ passive
681 sampling technology utilising diffusive pore water equilibration offers a possible means to address this
682 scale gap. Dialysis 'peepers' can provide high-resolution solute profiles using a chambered sampler
683 design (Lewandowski et al., 2002; Tan et al., 2005) and have been used to investigate CE plume fate at
684 centimetre-scale (Lorah and Olsen, 1999; LaSage et al., 2008). Peepers require up to several weeks for
685 concentration equilibration to be achieved between ambient pore water and dialysis cell water during
686 which the sampler is vulnerable to disturbance and transient effects (Tan et al., 2005). Simsir et al.
687 (2017) used direct push diffusion samplers (Fig. 6) comprised of glass vials with polyethene or non-
688 woven porous fabric deployed into shallow creek sediment in Tennessee which were equilibrated for
689 two weeks. Passive sampling technology using hydrogel media requires much shorter equilibration
690 times (24-72 hours) and offers a promising way forward to address the mm monitoring scale gap.
691 Diffusive equilibration or gradient sampling in thin films (DET/DGT) has provided mm-scale depth
692 profiles of inorganic nitrogen species, phosphorus and metals in stream sediments (Davison et al., 1994;
693 Palmer-Felgate et al., 2010; Ullah et al., 2012). This technology has recently been applied to studies of

694 enhanced attenuation of groundwater nitrate in riverbeds influenced by in-stream vegetation growth
695 (Ullah et al., 2014). As Briggs et al. (2015) duly point out, extractive sampling procedures tend to always
696 bias the mobile porosity domain of reactive sediment zones which is overcome by diffusive thin film
697 approaches. This technology offers the best opportunity to capture vertical scales approaching the size
698 of pore networks where key reactive transport features such as anoxic microzones may be resolved. As
699 such, this technology can provide a nested observational capability when combined with larger scale
700 solute profiles for a more integrated understanding of plume behaviour.

701 Given that microbial biomass occurs predominantly as biofilms, microbial sampling in the
702 hyporheic zone is sensitive to particle size distribution given that the surface area available for
703 colonisation decreases with increasing particle size (Mendoza-Lera et al., 2017). Direct sampling of fine
704 sediment fractions for molecular analyses of microbial composition have been taken from surficial
705 sediment layers using piston corers (Atashgahi et al., 2012; Hamonts et al., 2014; Vandermeeren et al.,
706 2014) as well as high resolution sub-sampling of deeper cores (Abe et al., 2009; Atashgahi et al., 2014).
707 These methods are well suited to homogenous silt and clay sediments but are subject to the same
708 limitations for coring in granular deposits discussed above. Microbial 'trapping' using an emplaced
709 porous medium for biofilm colonisation is an established approach in aquifer media (Voisin et al., 2016).
710 At the Tennessee creek, Simsir et al. (2017) were able to measure in-situ changes in microbial
711 community structure at high spatial resolution using Bio-Sep bead traps (www.microbe.com) arranged
712 along a 55 cm vertical profile. By combining microbial and pore water sampling (Fig. 6), their work
713 permitted a comprehensive picture of microbial community structure and biogeochemical gradients to
714 be formed. This approach can offer unique insights on linkages between chemical and microbial factors
715 which govern in-situ biotransformation capacity and is suitable for deployment at a range of scales.

716 ## 4 Conclusions and outlook

717 ### 4.1 Conclusions

718 Our review has established the degree to which hyporheic zones can serve as natural bioreactors
719 capable of reducing mass fluxes of CEs to surface water from groundwater sources. Although OHRB
720 appear to be relatively widespread in riverbeds, field experience to date has shown that in-situ anoxic

721 biotransformation tends to be patchy (Table 1) where fine-grained or SOM-rich sediments occur (Fig
722 1). Observed transformation extents range from partial TCE to cDCE dechlorination to near-complete
723 stoichiometric conversion of TCE to ethene (Fig. 6). In DOM-dominated foodwebs, OHR requires
724 residence times along discharging groundwater flow paths to exceed the reaction timescales for higher-
725 energy TEAs such as O_2 and nitrate. Here, extracellular H_2 will be closely regulated by interspecies
726 transfers between fermenters and heterotrophs (Fig. 3) such as OHRB and methanogens. Competitive
727 interactions between dechlorinators and mineral reducing TEAPs (particularly sulfate) may inhibit OHR
728 steps, particularly cDCE to VC and VC to ethene (Fig. 4). When H_2 is limiting, OHR may compete with
729 these TEAPs for reducing power. Toxic metabolite formation (e.g. sulfide) may cause inhibition when
730 H_2 is unlimited. Conversely, syntrophic partnerships may develop between OHRB and other
731 hydrogenotrophs which may enhance in-situ biotransformation.

732 Thin mixing zones developing between discharging groundwater and downwelling surface water
733 carrying O_2 may create a dynamic anoxic-oxic interface potentially supporting ethenotrophs,
734 methanotrophs and ammonia oxidisers (Fig. 5). Here, a secondary niche environment for VC
735 mineralisation and to some extent, cDCE via direct metabolism and co-metabolism (from the action of
736 mono-oxygenase enzymes) can complete a coupled anoxic-oxic natural 'treatment' process. The oxic
737 potential of CE attenuation in hyporheic zones has only in the last few years become appreciated but is
738 not widely demonstrated at field scale. The efficacy of this step in the process will be dependent on the
739 presence of suitable aerobes and the thickness of mixing zones relative to discharging groundwater flow
740 paths transporting LCEs and co-substrates such as methane and ammonium produced from DOM
741 metabolism.

742 For both anoxic and oxic zone processes, mass transformation will be controlled by the sediment
743 surface area available for biofilm colonisation, delivery rates of critical reactants (e.g. H_2 or O_2), their
744 reaction timescales and exposure time in reactive zones. Diffusion-limited mass transfer from bulk pore
745 water to biofilm domains is likely to be the most important rate-limiting step governing in-situ
746 biotransformation efficacies. At pore scales, heterogeneity in pore throat size can induce dual mobility
747 porosity domains. Solute exposure timeframes are increased in the less mobile domain where anoxic

748 microsite formation may play an important role in the cumulative impact of processes.

749 Effective in-situ monitoring of hyporheic processes in plume discharge zones necessitates a
750 detailed conceptual understanding of the spatial and temporal variability of water flows and residence
751 times. This is best accomplished using non-invasive hydrogeophysical technologies and the application
752 of heat as a surrogate for advection where overlapping spatial scales may be observed simultaneously.
753 Bulk chemical gradients may be delineated using multi-level profiles with vertical resolutions of 0.1–
754 0.2 m often proving sufficient. Nested monitoring is warranted at critical boundary zones where the
755 local properties of pore networks may exert important cumulative controls on observed
756 biotransformation capacities. Simultaneous microbial and pore water sampling can demonstrate that
757 niche conditions for biotransformation are occurring in-situ and is advocated further.

758 **4.2 Future research opportunities**

759 Additional field experience is required to better address spatial and temporal biotransformation
760 variability and allow predictive models to be developed. Directions to improve the current conceptual
761 understanding are outlined as follows:

762 • Integrated field studies addressing coupled flow and reactive transport along pathways at
763 multiple scales are needed (Oldham et al., 2013; Pinay et al., 2015; Abbot et al., 2016). New in-
764 situ tools have emerged which can quantify residence times at high spatial resolution (e.g. Rønde
765 et al., 2017). Dual reactive-conservative 'smart' tracer studies such as acetate-bromide (Rinehart
766 et al., 2015), acetate-resazurin-resorufin (Briggs et al., 2013) which can quantify both residence
767 time and reaction timescales for TEA-DOC couples offer an integrated way forward.

768 • Capturing in-situ spatial and temporal dynamics of O_2/H_2 gradients along discharging
769 groundwater flow paths. These key end-members alone can provide the critical diagnostic
770 information on redox status and indications of key tipping points and priming events which
771 govern in-situ anaerobic-aerobic biotransformation efficacies.

772 • Finally, these recent advances should be coupled with microbiological studies to better
773 understand the ecophysiology of anaerobic and aerobic CE-transforming microbes and their

interaction with biotic and abiotic factors. Overall, interdisciplinary efforts are necessary to enhance understanding of hydrological, chemical, physical and microbial interactions and critical gradients that influence the fate of CE in hyporheic zones.

Acknowledgments

The research of J. Weatherill has been supported by Keele University's ACORN scheme and the UK Environment Agency. The research of S. Atashgahi is supported by a grant of BE-Basic-FES funds from the Dutch Ministry of Economic Affairs. The work of S. Krause has been supported by funds from grant NERC-NE/I016120/1. The authors would like to acknowledge Jeff Roberts (SiREM Lab, Canada) for his helpful comments on our original manuscript. We would like to kindly thank Poul Bjerg (Technological University of Denmark) and two anonymous reviewers for their constructive and thoughtful comments to help improve our paper.

5 References

Abbott, B.W., Baranov, V., Mendoza-Lera, C., Nikolakopoulou, M., Harjung, A., Kolbe, T., Balasubramanian, M.N., Vaessen, T.N., Ciocca, F., Campeau, A., Wallin, M.B., 2016. Using multi-tracer inference to move beyond single-catchment ecohydrology. Earth-Sci. Rev. 160, 19–42.

Abe, Y., Aravena, R., Zopfi, J., Parker, B., Hunkeler, D., 2009. Evaluating the fate of chlorinated ethenes in streambed sediments by combining stable isotope, geochemical and microbial methods. J. Contam. Hydrol. 107 (1) 10–21.

Allen-King, R.M., Grathwohl, P., Ball, W.P., 2002. New modeling paradigms for the sorption of hydrophobic organic chemicals to heterogeneous carbonaceous matter in soils, sediments, and rocks. Adv. Water Resour. 25 (8) 985−1016.

Angermann, L., Krause, S., Lewandowski, J., 2012. Application of heat pulse injections for investigating shallow hyporheic flow in a lowland river. Water Resour. Res. 48 (12) W00P02.

Anibas, C., Buis, K., Verhoeven, R., Meire, P., Batelaan, O., 2011. A simple thermal mapping method for seasonal spatial patterns of groundwater–surface water interaction. J. Hydrol. 397 (1) 93–104.

799 Anibas, C., Schneidewind, U., Vandersteen, G., Joris, I., Seuntjens, P., Batelaan, O., 2016. From
800 streambed temperature measurements to spatial-temporal flux quantification: Using the LPML method
801 to study groundwater-surface water interaction. Hydrol. Process. 30 203–216.

802 Arciero, D., Vannelli, T., Logan, M., Hopper, A.B., 1989. Degradation of trichloroethylene by the
803 ammonia-oxidizing bacterium *Nitrosomonas europaea*. Biochem. Biophys. Res. Commun. 159 (2) 640–
804 643.

805 Arp, D.J., 1995. Understanding the diversity of trichloroethene co-oxidations. Curr. Opin. Biotechnol.
806 6 (3) 352–358.

807 Atashgahi, S., Aydin, R., Dimitrov, M.R., Sipkema, D., Hamonts, K., Lahti, L., Maphosa, F., Kruse, T.,
808 Saccenti, E., Springael, D., Dejonghe, W., 2015. Impact of a wastewater treatment plant on microbial
809 community composition and function in a hyporheic zone of a eutrophic river. Sci. Rep. 5: 17284.

810 Atashgahi, S., Lu, Y., Ramiro-Garcia, J., Peng, P., Maphosa, F., Sipkema, D., Dejonghe, W., Smidt, H.,
811 Springael, D., 2017a. Geochemical parameters and reductive dechlorination determine aerobic
812 cometabolic vs aerobic metabolic vinyl chloride biodegradation at oxic/anoxic interface of hyporheic
813 zones. Environ. Sci. Technol. 51 (3) 1626–1634.

814 Atashgahi, S., Lu, Y., Smidt, H., 2016. Overview of known organohalide-respiring
815 bacteria−phylogenetic diversity and environmental distribution. In: Lorenz., A., Löffler, F., (Eds.)
816 Organohalide-Respiring Bacteria. Springer Berlin, Heidelberg, pp. 63−105.

817 Atashgahi, S., Maphosa, F., De Vrieze, J., Haest, P.J., Boon, N., Smidt, H., Springael, D., Dejonghe,
818 W., 2014. Evaluation of solid polymeric organic materials for use in bioreactive sediment capping to
819 stimulate the degradation of chlorinated aliphatic hydrocarbons. Appl. Microbiol. Biotechnol. 98 (5)
820 2255–2266.

821 Atashgahi, S., Maphosa, F., Doğan, E., Smidt, H., Springael, D. and Dejonghe, W., 2013. Small-scale
822 oxygen distribution determines the vinyl chloride biodegradation pathway in surficial sediments of
823 riverbed hyporheic zones. FEMS Microbiol. Ecol. 84 (1) 133–142.

824 Atashgahi. S., Lu, Y., Zheng, Y., Saccenti, E., Suarez-Diez, M., Ramiro Garcia, J., Eisenmann, H.,
825 Elsner, M., Stams, A.J.M., Springael, D., Dejonghe, W., Smidt, H. 2017b. Geochemical and microbial
826 community determinants of reductive dechlorination at a site biostimulated with glycerol. Environ.
827 Microbiol. 19 968–981.

828 Aulenta, F., Beccari, M., Majone, M., Papini, M.P., Tandoi, V., 2008. Competition for H_2 between
829 sulfate reduction and dechlorination in butyrate-fed anaerobic cultures. Process Biochem. 43 (2) 161–
830 168.

831 Aulenta, F., Majone, M., Verbo, P., Tandoi, V., 2002. Complete dechlorination of tetrachloroethene to
832 ethene in presence of methanogenesis and acetogenesis by an anaerobic sediment microcosm.
833 Biodegradation 13 (6) 411−424.

834 Aulenta, F., Pera, A., Rossetti, S., Papini, M.P., Majone, M., 2007. Relevance of side reactions in
835 anaerobic reductive dechlorination microcosms amended with different electron donors. Water Res. 41
836 (1) 27−38.

837 Azizian, M.F., Marshall, I.P., Behrens, S., Spormann, A.M., Semprini, L., 2010. Comparison of lactate,
838 formate, and propionate as hydrogen donors for the reductive dehalogenation of trichloroethene in a
839 continuous-flow column. J. Cont. Hydrol. 113 (1) 77−92.

840 Bagley, D.M., Gossett, J.M., 1990. Tetrachloroethene transformation to trichloroethene and cis-1, 2-
841 dichloroethene by sulfate-reducing enrichment cultures. Appl. Environ. Microbiol. 56 (8) 2511−2516.

842 Baker, M.A., Dahm, C.N., Valett, H.M., 1999. Acetate retention and metabolism in the hyporheic zone
843 of a mountain stream. Limnol. Oceanogr. 44 (6) 1530–1539.

844 Baker, M.A., Valett, H.M., Dahm, C.N., 2000. Organic carbon supply and metabolism in a shallow
845 groundwater ecosystem. Ecol. 81 (11) 3133–3148.

846 Baker, M.A., Vervier, P., 2004. Hydrological variability, organic matter supply and denitrification in
847 the Garonne River ecosystem. Freshwater Biol. 49 (2) 181−190.

848 Ballapragada, B.S., Stensel, H.D., Puhakka, J.A., Ferguson, J.F., 1997. Effect of hydrogen on reductive
849 dechlorination of chlorinated ethenes. Environ. Sci. Technol. 31 (6) 1728−1734.

850 Battin, T.J., 1997. Assessment of fluorescein diacetate hydrolysis as a measure of total esterase activity
851 in natural stream sediment biofilms. Sci. Total Environ. 198 (1) 51–60.

852 Battin, T.J., Besemer, K., Bengtsson, M.M., Romani, A.M., Packmann, A.I., 2016. The ecology and
853 biogeochemistry of stream biofilms. Nat. Rev. Microbiol. 14 (4) 251–263.

854 Battin, T.J., Kaplan, L.A., Findlay, S., Hopkinson, C.S., Marti, E., Packman, A.I., Newbold, J.D.,
855 Sabater, F., 2008. Biophysical controls on organic carbon fluxes in fluvial networks. Nat. Geosci. 1 (2)
856 95–100.

857 Battin, T.J., Kaplan, L.A., Newbold, J.D., Hansen, C.M., 2003. Contributions of microbial biofilms to
858 ecosystem processes in stream mesocosms. Nature 426 (6965) 439–442.

859 Bengtsson, M.M., Wagner, K., Burns, N.R., Herberg, E.R., Wanek, W., Kaplan, L.A., Battin, T.J., 2014.
860 No evidence of aquatic priming effects in hyporheic zone microcosms. Sci. Rep. 4 5187.

861 Benker, E., Davis, G.B., Appleyard, S., Barry, D.A., Power, T.R., 1996. Trichloroethene (TCE)
862 contamination in an unconfined sand aquifer underlying a residential area of Perth, Western Australia.
863 Hydrogeol. J. 4 (1) 20–29.

864 Berggren, D.R., Marshall, I.P., Azizian, M.F., Spormann, A.M., Semprini, L., 2013. Effects of sulfate
865 reduction on the bacterial community and kinetic parameters of a dechlorinating culture under chemostat
866 growth conditions. Environ. Sci. Technol. 47 (4) 1879−1886.

867 Binley, A., Ullah, S., Heathwaite, A.L., Heppell, C., Byrne, P., Lansdown, K., Trimmer, M., Zhang, H.,
868 2013. Revealing the spatial variability of water fluxes at the groundwater-surface water interface. Water
869 Resour. Res. 49 (7) 3978–3992.

870 Boano, F., Harvey, J.W., Marion, A., Packman, A.I., Revelli, R., Ridolfi, L., Wörman, A., 2014.
871 Hyporheic flow and transport processes: Mechanisms, models, and biogeochemical implications. Rev.
872 Geophys. 52 (4) 603–679.

873 Böhlke, J.K., O'Connell, M.E., Prestegaard, K.L., 2007. Ground water stratification and delivery of
874 nitrate to an incised stream under varying flow conditions. J. Environ. Qual. 36 (3) 664–680.

875 Bommer, M., Kunze, C., Fesseler, J., Schubert, T., Diekert, G., Dobbek, H., 2014. Structural basis for
876 organohalide respiration. Science, 346 (6208) 455−458.

877 Boopathy, R., Peters, R., 2001. Enhanced biotransformation of trichloroethylene under mixed electron
878 acceptor conditions. Current Microbiol. 42 (2) 134−138.

879 Boulton, A.J., Findlay, S., Marmonier, P., Stanley, E.H., Valett, H. M., 1998. The functional significance
880 of the hyporheic zone in streams and rivers. Ann. Rev. Ecol. Syst. 29 59–81.

881 Brablcova, L., Buriánková, I., Badurova, P., Chaudhary, P.P., Rulik, M., 2015. Methanogenic archaea
882 diversity in hyporheic sediments of a small lowland stream. Anaerobe. 32 24−31.

883 Bradley, P., Chapelle, F., 1998b. Microbial mineralization of VC and DCE under different terminal
884 electron accepting conditions. Anaerobe, 4 (2) 81–87.

885 Bradley, P.M., Chapelle, F.H., 1998a. Effect of contaminant concentration on aerobic microbial
886 mineralization of DCE and VC in stream-bed sediments. Environ. Sci. Technol. 32 (5) 553−557.

887 Bradley, P.M., Chapelle, F.H., 2000. Aerobic microbial mineralization of dichloroethene as sole carbon
888 substrate. Environ. Sci. Technol. 34 (1) 221−223.

889 Bradley, P.M., Chapelle, F.H., 2011. Microbial mineralization of dichloroethene and vinyl chloride
890 under hypoxic conditions. Groundwater Monit. Remediat. 31 (4) 39–49.

891 Briggs, M.A., Buckley, S.F., Bagtzoglou, A.C., Werkema, D.D., Lane, J.W., 2016. Actively heated
892 high-resolution fiber-optic-distributed temperature sensing to quantify streambed flow dynamics in
893 zones of strong groundwater upwelling. Water Resour. Res. 52 (7) 5179–5194.

894 Briggs, M.A., Day-Lewis, F.D., Ong, J.B., Harvey, J.W., Lane, J.W., 2014. Dual-domain mass-transfer
895 parameters from electrical hysteresis: Theory and analytical approach applied to laboratory, synthetic
896 streambed, and groundwater experiments. Water Resour. Res. 50 (10) 8281–8299.

897 Briggs, M.A., Day-Lewis, F.D., Zarnetske, J.P., Harvey, J.W., 2015. A physical explanation for the
898 development of redox microzones in hyporheic flow. Geophys. Res. Lett. 42 (11) 4402–4410.

899 Briggs, M.A., Lautz, L.K., Hare, D.K., 2014. Residence time control on hot moments of net nitrate
900 production and uptake in the hyporheic zone. Hydrol. Process. 28 (11) 3741–3751.

901 Briggs, M.A., Lautz, L.K., Hare, D.K., González-Pinzón, R., 2013. Relating hyporheic fluxes, residence
902 times, and redox-sensitive biogeochemical processes upstream of beaver dams. Freshwater Sci. 32 (2)
903 622−641.

904 Burk, L., Cook, P.G., 2015. A simple and affordable system for installing shallow drive point
905 piezometers. Groundwater Monit. Remediat. 35 (3) 101–104.

906 Burston, M.W., Nazari, M.M., Bishop, P.K., Lerner, D.N., 1993. Pollution of groundwater in the
907 Coventry region (UK) by chlorinated hydrocarbon solvents. J. Hydrol. 149 (1–4), 137–161.

908 Buss, S., Cai, Z., Cardenas, B., Fleckenstein, J., Hannah, D., Heppell, K., Hulme, P., Ibrahim, T.,
909 Kaeser, D., Krause, S., Lawler, D., Lerner, D., Mant, J., Malcolm, I., Old, G., Parkin, G., Pickup, R.,
910 Pinay, G., Porter, J., Rhodes, G., Richie, A., Riley, J., Robertson, A.L., Sear, D., Shields, B., Smith,
911 J., Tellam, J., Wood, P., 2009. The Hyporheic Handbook: A handbook on the groundwater -
912 surface-water interface and ecology of the hyporheic zone for environmental managers. Environment
913 Agency Science Report SC0 50070. Environment Agency, Bristol, UK.

914 Byrne, P., Binley, A., Heathwaite, A.L., Ullah, S., Heppell, C.M., Lansdown, K., Zhang, H., Trimmer,
915 M., Keenan, P., 2014. Control of river stage on the reactive chemistry of the hyporheic zone. Hydrol.
916 Process. 28 (17) 4766–4779.

917 Caccavo, F., Jr., Blakemore, R.P., Lovley, D.R., 1992. A hydrogen-oxidizing, Fe(III)-reducing
918 microorganism from the Great Bay estuary, New Hampshire. Appl. Environ. Microbiol. 58 3211–3216.

919 Cardenas, M.B., 2009. Stream-aquifer interactions and hyporheic exchange in gaining and losing
920 sinuous streams. Water Resour. Res. 45 (6) W06429.

921 Cardenas, M.B., 2015. Hyporheic zone hydrologic science: A historical account of its emergence and a
922 prospectus. Water Resour. Res. 51 (5) 3601–3616.

923 Cardenas, M.B., Ford, A.E., Kaufman, M.H., Kessler, A.J., Cook, P.L., 2016. Hyporheic flow and
924 dissolved oxygen distribution in fish nests: The effects of open channel velocity, permeability patterns,
925 and groundwater upwelling. J. Geophys. Res. Biogeosci. 121 (12) 3113–3130.

926 Chambon, J.C., Bjerg, P.L., Scheutz, C., Bælum, J., Jakobsen, R., Binning, P.J., 2013. Review of
927 reactive kinetic models describing reductive dechlorination of chlorinated ethenes in soil and
928 groundwater. Biotechnol. Bioeng, 110 (1) 1−23.

929 Chambon, J.C., Broholm, M.M., Binning, P.J. Bjerg, P.L. 2010. Modeling multi-component transport
930 and enhanced anaerobic dechlorination processes in a single fracture-clay matrix system. J. Cont.
931 Hydrol. 112 77−90.

932 Chan, B., Radom, L., 2011. Assessment of theoretical procedures for hydrogen-atom abstraction by
933 chlorine, and related reactions. Theor. Chem. Acc. 130 (2-3) 251−260.

934 Chan, W.W., Grostern, A., Löffler, F.E., Edwards, E.A., 2011. Quantifying the effects of 1,1,1-
935 trichloroethane and 1,1-dichloroethane on chlorinated ethene reductive dehalogenases. Environ. Sci.
936 Technol. 45 (22) 9693−9702.

937 Chapelle, F.H., Bradley, P.M., McMahon, P.B., Kaiser, K., Benner, R., 2012. Dissolved oxygen as an
938 indicator of bioavailable dissolved organic carbon in groundwater. Ground Water 50 (2) 230–241.

939 Chapman, S.W., Parker, B.L., Cherry, J.A., Aravena, R. Hunkeler, D., 2007. Groundwater–surface
940 water interaction and its role on TCE groundwater plume attenuation. J. Contam. Hydrol. 91 (3) 203–
941 232.

942 Chen, I.M., Chang, B.V., Yuan, S.Y., Wang, Y.S., 2002. Reductive dechlorination of
943 hexachlorobenzene under various additions. Water Air Soil Pollut. 139 (1) 61−74.

944 Christof, O., Seifert, R., Michaelis, W., 2002. Volatile halogenated organic compounds in European
945 estuaries. Biogeochemistry, 59 (1) 143–160.

946 Chung, J., Rittmann, B.E., 2008. Simultaneous bio-reduction of trichloroethene, trichloroethane, and
947 chloroform using a hydrogen-based membrane biofilm reactor. Water Sci. Technol. 58 (3) 495−501.

948 Coleman, N.V., Mattes, T.E., Gossett, J.M., Spain, J.C., 2002. Biodegradation of cis-dichloroethene as
949 the sole carbon source by a β-proteobacterium. Appl. Environ. Microbiol. 68 (6) 2726−2730.

950 Conant, B., 2004. Delineating and quantifying ground water discharge zones using streambed
951 temperatures. Ground water, 42 (2) 243–257.

952 Conant, B., Cherry, J.A. Gillham, R.W., 2004. A PCE groundwater plume discharging to a river:
953 influence of the streambed and near-river zone on contaminant distributions. J. Contam. Hydrol. 73 (1)
954 249–279.

955 Conrad, M.E., Brodie, E.L., Radtke, C.W., Bill, M., Delwiche, M.E., Lee, M.H., Swift, D.L., Colwell,
956 F.S., 2010. Field evidence for co-metabolism of trichloroethene stimulated by addition of electron donor
957 to groundwater. Environ. Sci. Technol. 44 (12) 4697–4704.

958 Cord-Ruwisch, R., Seitz, H.-J., Conrad, R., 1988. The capacity of hydrogenotrophic bacteria to compete
959 for traces of hydrogen depends on the redox potential of the terminal electron acceptor. Arch. Microbiol.
960 149 350–357.

961 Cuthbert, M.O., Mackay, R., Durand, V., Aller, M.F., Greswell, R.B., Rivett, M.O., 2010. Impacts of
962 river bed gas on the hydraulic and thermal dynamics of the hyporheic zone. Adv. Water Resour. 33 (11)
963 1347–1358.

964 Danko, A.S., Luo, M., Bagwell, C.E., Brigmon, R.L., Freedman, D.L., 2004. Involvement of linear
965 plasmids in aerobic biodegradation of vinyl chloride. Appl. Environ. Microbiol. 70 (10) 6092−6097.

966 Davey, M.E., O'Toole, G.A., 2000. Microbial biofilms: from ecology to molecular genetics. Microbiol.
967 Mol. Biol. Rev. 64 (4) 847–867.

968 Davison, W., Zhang, H., Grime, G. W., 1994. Performance characteristics of gel probes used for
969 measuring the chemistry of pore waters. Environ. Sci. Technol. 28 1623–1632.

970 Descloux, S., Datry, T., Philippe, M., Marmonier, P., 2010. Comparison of different techniques to assess
971 surface and subsurface streambed colmation with fine sediments. Int. Rev. Hydrobiol. 95 (6) 520–540.

Diekert, G., Wohlfarth, G., 1994. Metabolism of homoacetogens. Antonie van Leeuwenhoek, 66 (1) 209–221.

Dolfing, J., Beurskens, J. E. M., 1995. The microbial logic and environmental significance of reductive dehalogenation. In: Jones, J.G., (Ed.), Advances in microbial ecology 14, Plenum Press, New York, pp 143–206.

Donn, M.J., Barron, O.V., 2013. Biogeochemical processes in the groundwater discharge zone of urban streams. Biogeochemistry 115 (1-3) 267–286.

Duhamel, M., Wehr, S.D., Yu, L., Rizvi, H., Seepersad, D., Dworatzek, S., Cox, E.E., Edwards, E.A., 2002. Comparison of anaerobic dechlorinating enrichment cultures maintained on tetrachloroethene, trichloroethene, cis-dichloroethene and vinyl chloride. Water Res. 36 (17) 4193−4202.

Dupont, R.R., Sorensen, D.L., McLean, J.E., Doucette, B.J., Loucks, M., 2003. Enhancement of trichloroethylene degradation via carbon donor and microbial amendment addition. In: Magar, V.S., Kelley, M.E., (Eds.), Proceedings of the Seventh International In Situ and On-site Bioremediation Symposium, Orlando, Florida, USA, 25 June 2003. Battelle Press, Columbus, OH, p. A-26.

Egli, T., 2010. How to live at very low substrate concentration. Water Res. 44 (17) 4826–4837.

Elango, V.K., Liggenstoffer, A.S., Fathepure, B.Z., 2006. Biodegradation of vinyl chloride and cis-dichloroethene by a *Ralstonia* sp. strain TRW-1. Appl. Microbiol. Biotechnol. 72 (6) 1270−1275.

Ellis, P.A., Rivett, M.O., 2007. Assessing the impact of VOC-contaminated groundwater on surface water at the city scale. J. Contam. Hydrol. 91 (1) 107–127.

Fennell, D.E., Gossett, J.M., Zinder, S.H., 1997. Comparison of butyric acid, ethanol, lactic acid, and propionic acid as hydrogen donors for the reductive dechlorination of tetrachloroethene. Environ. Sci. Technol. 31 (3) 918–926.

Findlay, M., Smoler, D.F., Fogel, S. Mattes, T.E., 2016. Aerobic vinyl chloride metabolism in groundwater microcosms by methanotrophic and etheneotrophic bacteria. Environ. Sci. Technol. 50 (7) 3617–3625.

997 Findlay, S.E., Sinsabaugh, R.L., Sobczak, W.V., Hoostal, M., 2003. Metabolic and structural response
998 of hyporheic microbial communities to variations in supply of dissolved organic matter. Limnol.
999 Oceanogr. 48 (4) 1608–1617.

1000 Fischer, H., Kloep, F., Wilzcek, S., Pusch, M.T., 2005. A river's liver–microbial processes within the
1001 hyporheic zone of a large lowland river. Biogeochemistry 76 (2) 349–371.

1002 Fleckenstein, J.H., Niswonger, R.G., Fogg, G.E., 2006. River-aquifer interactions, geologic
1003 heterogeneity, and low-flow management. Ground water, 44 (6) 837–852.

1004 Forrester, S.B., Han, J.I., Dybas, M.J., Semrau, J.D., Lastoskie, C.M., 2005. Characterization of a mixed
1005 methanotrophic culture capable of chloroethylene degradation. Environ. Eng. Sci. 22 (2) 177–186.

1006 Fox, A., Boano, F., Arnon, S., 2014. Impact of losing and gaining streamflow conditions on hyporheic
1007 exchange fluxes induced by dune-shaped bed forms. Water Resour. Res. 50 (3) 1895−1907.

1008 Franken, R.J., Storey, R.G., Williams, D.D., 2001. Biological, chemical and physical characteristics of
1009 downwelling and upwelling zones in the hyporheic zone of a north-temperate stream. Hydrobiologia,
1010 444 (1-3) 183–195.

1011 Freitas, J.G., Rivett, M.O., Roche, R.S., Durrant, M., Walker, C., Tellam, J.H., 2015. Heterogeneous
1012 hyporheic zone dechlorination of a TCE groundwater plume discharging to an urban river reach. Sci.
1013 Total Environ. 505 236–252.

1014 Freixa, A., Rubol, S., Carles-Brangarí, A., Fernàndez-Garcia, D., Butturini, A., Sanchez-Vila, X.,
1015 Romaní, A.M., 2016. The effects of sediment depth and oxygen concentration on the use of organic
1016 matter: an experimental study using an infiltration sediment tank. Sci. Total Environ. 540 20–31.

1017 Fryar, A.E., Wallin, E.J., Brown, D.L., 2000. Spatial and temporal variability in seepage between a
1018 contaminated aquifer and tributaries to the Ohio River. Groundwater Monit. Remediat. 20 (3) 129–146.

1019 Fullerton, H., Rogers, R., Freedman, D.L., Zinder, S.H., 2014. Isolation of an aerobic vinyl chloride
1020 oxidizer from anaerobic groundwater. Biodegradation 25 (6) 893−901.

1021 Gavala, H.N., Angelidaki, I., Ahring, B.K., 2003. Kinetics and modeling of anaerobic digestion process.
1022 In: Ahring, B.K. (Ed.) Biomethanation I. Springer Berlin Heidelberg, pp. 57–93.

1023 Gette-Bouvarot, M., Mermillod-Blondin, F., Lemoine, D., Delolme, C., Danjean, M., Etienne, L. and
1024 Volatier, L., 2015. The potential control of benthic biofilm growth by macrophytes—A mesocosm
1025 approach. Ecol. Eng. 75 178–186.

1026 Giovannini, G., Donoso-Bravo, A., Jeison, D., Chamy, R., Ruíz-Filippi, G., Wouwer, A.V., 2016. A
1027 review of the role of hydrogen in past and current modelling approaches to anaerobic digestion
1028 processes. Int. J. Hydrogen Energy 41 (39) 17713−17722.

1029 Gomez-Velez, J.D., Krause, S., Wilson, J.L., 2014. Effect of low-permeability layers on spatial patterns
1030 of hyporheic exchange and groundwater upwelling. Water Resour. Res. 50 (6) 5196–5215.

1031 González-Pinzón, R., Ward, A.S., Hatch, C.E., Wlostowski, A.N., Singha, K., Gooseff, M.N., Haggerty,
1032 R., Harvey, J.W., Cirpka, O.A., Brock, J.T., 2015. A field comparison of multiple techniques to quantify
1033 groundwater–surface-water interactions. Freshwater Sci. 34 (1) 139–160.

1034 Gossett, J.M., 2010. Sustained aerobic oxidation of vinyl chloride at low oxygen concentrations.
1035 Environ. Sci. Technol. 44 (4) 1405–1411.

1036 Haest, P.J., Philips, J., Springael, D., Smolders, E., 2011. The reactive transport of trichloroethene is
1037 influenced by residence time and microbial numbers. J. Cont. Hydrol. 119 (1) 89–98.

1038 Haggerty, R., Wondzell, S.M., Johnson, M.A., 2002. Power-law residence time distribution in the
1039 hyporheic zone of a 2nd-order mountain stream. Geophys. Res. Let. 29 (13) 18-1–18-4.

1040 Hallenbeck, P.C., Ghosh, D., 2009. Advances in fermentative biohydrogen production: the way
1041 forward? Trends Biotechnol. 27 (5) 287–297.

1042 Hamonts, K., Kuhn, T., Maesen, M., Bronders, J., Lookman, R., Kalka, H., Diels, L., Meckenstock,
1043 R.U., Springael, D., Dejonghe, W., 2009. Factors determining the attenuation of chlorinated aliphatic
1044 hydrocarbons in eutrophic river sediment impacted by discharging polluted groundwater. Environ. Sci.
1045 Technol. 43 (14) 5270–5275.

1046 Hamonts, K., Ryngaert, A., Maesen, M., Vos, J., Wilzcek, D., Bronders, J., Diels, L., Dejonghe, W.,
1047 Dijk, J., Springael, D., Sturme, M., 2007. Sediment biobarriers for chlorinated aliphatic hydrocarbons
1048 in groundwater reaching surface water (SEDBARCAH Project). In: Hull R.N., Barbu CH., Goncharova
1049 N. (Eds.) Strategies to enhance environmental Security in Transition Countries. NATO Science for
1050 Peace and Security Series C: Environmental Security. Springer, Dordrecht, pp. 249–261.

1051 Hamonts, K., Ryngaert, A., Smidt, H., Springael, D., Dejonghe, W., 2014. Determinants of the microbial
1052 community structure of eutrophic, hyporheic river sediments polluted with chlorinated aliphatic
1053 hydrocarbons. FEMS Microbial. Ecol. 87 (3) 715−732.

1054 Harkness, M., Fisher, A., Lee, M.D., Mack, E.E., Payne, J.A., Dworatzek, S., Roberts, J., Acheson, C.,
1055 Herrmann, R., Possolo, A., 2012. Use of statistical tools to evaluate the reductive dechlorination of high
1056 levels of TCE in microcosm studies. J. Cont. Hydrol. 131 (1) 100−118.

1057 Hartmans, S., De Bont, J.A., 1992. Aerobic vinyl chloride metabolism in *Mycobacterium aurum* L1.
1058 Appl. Environ. Microbiol. 58 (4) 1220−1226.

1059 Hartmans, S., De Bont, J.A.M., Tramper, J., Luyben, K.C.A., 1985. Bacterial degradation of vinyl
1060 chloride. Biotechnol. Let. 7 (6) 383−388.

1061 Harvey, J.W., Bencala, K.E., 1993. The effect of streambed topography on surface-subsurface water
1062 exchange in mountain catchments. Water Resour. Res. 29 (1) 89–98.

1063 He, J., Sung, Y., Dollhopf, M.E., Fathepure, B.Z., Tiedje, J.M., Löffler, F.E., 2002. Acetate versus
1064 hydrogen as direct electron donors to stimulate the microbial reductive dechlorination process at
1065 chloroethene-contaminated sites. Environ. Sci. Technol., 36 (18) 3945−3952.

1066 Heimann, A., Jakobsen, R., Blodau, C., 2009. Energetic constraints on H_2-dependent terminal electron
1067 accepting processes in anoxic environments: a review of observations and model approaches. Environ.
1068 Sci. Technol. 44 (1) 24–33.

1069 Heimann, A.C., Batstone, D.J., Jakobsen, R., 2006. Methanosarcina spp. drive vinyl chloride
1070 dechlorination via interspecies hydrogen transfer. Appl. Environ. Microbiol. 72 (4) 2942−2949.

1071 Helton, A.M., Ardón, M., Bernhardt, E.S., 2015. Thermodynamic constraints on the utility of ecological
1072 stoichiometry for explaining global biogeochemical patterns. Ecol. Lett. 18 (10) 1049–1056.

1073 Heppell, C., Heathwaite, A.L., Binley, A., Byrne, P., Ullah, S., Lansdown, K., Keenan, P., Trimmer,
1074 M., Zhang, H., 2014. Interpreting spatial patterns in redox and coupled water–nitrogen fluxes in the
1075 streambed of a gaining river reach. Biogeochemistry, 117 (2-3) 491−509.

1076 Hester, E.T., Cardenas, M.B., Haggerty, R., Apte, S.V., 2017. The importance and challenge of
1077 hyporheic mixing. Water Resour. Res. DOI: 10.1002/2016WR020005.

1078 Hester, E.T., Young, K.I., Widdowson, M.A., 2013. Mixing of surface and groundwater induced by
1079 riverbed dunes: Implications for hyporheic zone definitions and pollutant reactions. Water Resour. Res.
1080 49 (9) 5221−5237.

1081 Hlaváčová, E., Rulík, M., Čáp, L., 2005. Anaerobic microbial metabolism in hyporheic sediment of a
1082 gravel bar in a small lowland stream. River Res Appl. 21 (9) 1003−1011.

1083 Hoelen, T.P., Cunningham, J.A., Hopkins, G.D., Lebron, C.A., Reinhard, M., 2006. Bioremediation of
1084 cis-DCE at a sulfidogenic site by amendment with propionate. Groundwater Monit. Remediat. 26 (3)
1085 82−91.

1086 Hoelen, T.P., Reinhard, M., 2004. Complete biological dehalogenation of chlorinated ethylenes in
1087 sulfate containing groundwater. Biodegradation 15 (6) 395–403.

1088 Hoelen, T.P., Reinhard, M., 2004. Complete biological dehalogenation of chlorinated ethylenes in
1089 sulfate containing groundwater. Biodegradation 15 (6) 395−403.

1090 Horvath, R.S., 1972. Microbial co-metabolism and the degradation of organic compounds in nature.
1091 Bacteriol. Revs. 36 (2) 146.

1092 Huang, B., Lei, C., Wei, C., Zeng, G., 2014. Chlorinated volatile organic compounds (Cl–VOCs) in
1093 environment–sources, potential human health impacts, and current remediation technologies. Environ.
1094 Int. 71, 118–138.

1095 Hug, L.A., Maphosa, F., Leys, D., Löffler, F.E., Smidt, H., Edwards, E.A., Adrian, L., 2013. Overview
1096 of organohalide-respiring bacteria and a proposal for a classification system for reductive
1097 dehalogenases. Phil. Trans. R. Soc. B 368: 20120322.

1098 Jackson, R.E., 1998. The migration, dissolution, and fate of chlorinated solvents in the urbanized alluvial
1099 valleys of the southwestern USA. Hydrogeol. J. 6 (1), 144–155.

1100 Jahangir, M.M., Khalil, M.I., Johnston, P., Cardenas, L.M., Hatch, D.J., Butler, M., Barrett, M.,
1101 O'flaherty, V., Richards, K.G., 2012. Denitrification potential in subsoils: a mechanism to reduce nitrate
1102 leaching to groundwater. Agric. Ecosyst. Environ. 147 13−23.

1103 Jakobsen, R., Postma, D., 1999. Redox zoning, rates of sulfate reduction and interactions with Fe-
1104 reduction and methanogenesis in a shallow sandy aquifer, Rømø, Denmark. Geochim. Cosmochim.
1105 Acta. 63 (1) 137–151.

1106 Jin, Y. O., Mattes, T. E., 2008. Adaptation of aerobic, ethene assimilating *Mycobacterium* strains to
1107 vinyl chloride as a growth substrate. Environ. Sci. Technol. 42 (13) 4784−4789.

1108 Jobelius, C., Ruth, B., Griebler, C., Meckenstock, R.U., Hollender, J., Reineke, A., Frimmel, F.H.,
1109 Zwiener, C., 2011. Metabolites indicate hot spots of biodegradation and biogeochemical gradients in a
1110 high-resolution monitoring well. Environ. Sci. Technol. 45 (2) 474−481.Jones Jr, J.B., Fisher, S.G.,
1111 Grimm, N.B., 1995. Nitrification in the hyporheic zone of a desert stream ecosystem. J. N. Am. Benthol.
1112 Soc. 14 (2) 249–258.

1113 Jugder, B.E., Ertan, H., Bohl, S., Lee, M., Marquis, C.P., Manefield, M., 2016. Organohalide respiring
1114 bacteria and reductive dehalogenases: key tools in organohalide bioremediation. Front. Microbiol. 7:
1115 249.

1116 Jugder, B.E., Ertan, H., Lee, M., Manefield, M., Marquis, C.P., 2015. Reductive dehalogenases come of
1117 age in biological destruction of organohalides. Trends Biotechnol. 33 (10) 595−610.

1118 Justicia-Leon, S.D., Higgins, S., Mack, E.E., Griffiths, D.R., Tang, S., Edwards, E.A., Löffler, F.E.,
1119 2014. Bioaugmentation with distinct *Dehalobacter* strains achieves chloroform detoxification in
1120 microcosms. Environ. Sci. Technol. 48 (3) 1851−1858.

1121 Kalbus, E., Reinstorf, F., Schirmer, M., 2006. Measuring methods for groundwater-surface water
1122 interactions: a review. Hydrol. Earth Sys. Sci. Discuss. 10 (6) 873–887.

1123 Klier, N.J., West, R.J., Donberg, P.A., 1999. Aerobic biodegradation of dichloroethylenes in surface and
1124 subsurface soils. Chemosphere 38 (5) 1175−1188.

1125 Knapp, J.L., Osenbrück, K., Cirpka, O.A., 2015. Impact of non-idealities in gas-tracer tests on the
1126 estimation of reaeration, respiration, and photosynthesis rates in streams. Water Res. 83 205−216.

1127 Kocamemi, B.A., Çeçen, F., 2005. Cometabolic degradation of TCE in enriched nitrifying batch
1128 systems. J. Hazard. Mater. 125 (1) 260–265.

1129 Kocamemi, B.A., Çeçen, F., 2010. Biological removal of the xenobiotic trichloroethylene (TCE)
1130 through cometabolism in nitrifying systems. Bioresour. Technol. 101 (1) 430–433.

1131 Koch, J. Nowak, W., 2015. Predicting DNAPL mass discharge and contaminated site longevity
1132 probabilities: Conceptual model and high-resolution stochastic simulation. Water Resour. Res. 51 (2)
1133 806–831.

1134 Kranzioch, I., Stoll, C., Holbach, A., Chen, H., Wang, L., Zheng, B., Norra, S., Bi, Y., Schramm, K.W.,
1135 Tiehm, A., 2013. Dechlorination and organohalide-respiring bacteria dynamics in sediment samples of
1136 the Yangtze Three Gorges Reservoir. Environ. Sci. Pollut. Res. 20 (10) 7046−7056.

1137 Krause, S., Hannah, D.M., Fleckenstein, J.H., Heppell, C.M., Kaeser, D., Pickup, R., Pinay, G.,
1138 Robertson, A.L., Wood, P.J., 2011. Inter-disciplinary perspectives on processes in the hyporheic zone.
1139 Ecohydrol. 4 (4) 481–499.

1140 Krause, S., Klaar, M.J., Hannah, D.M., Mant, J., Bridgeman, J., Trimmer, M., Manning-Jones, S., 2014.
1141 The potential of large woody debris to alter biogeochemical processes and ecosystem services in lowland
1142 rivers. Wiley Interdiscip. Rev. Wat. (3) 263–275.

1143 Krause, S., Tecklenburg, C., Munz, M., Naden, E., 2013. Streambed nitrogen cycling beyond the
1144 hyporheic zone: flow controls on horizontal patterns and depth distribution of nitrate and dissolved
1145 oxygen in the upwelling groundwater of a lowland river. J. Geophys. Res. Biogeosci. 118 (1) 54–67.

1146 Krumholz, L.R., Sharp, R., Fishbain, S.S., 1996. A freshwater anaerobe coupling acetate oxidation to
1147 tetrachloroethylene dehalogenation. Appl. Environ. Microbiol. 62 (11) 4108−4113.

1148 Lapworth, D.J., Gooddy, D.C., Allen, D., Old, G.H., 2009. Understanding groundwater, surface water,
1149 and hyporheic zone biogeochemical processes in a Chalk catchment using fluorescence properties of
1150 dissolved and colloidal organic matter. J. Geophys. Res. Biogeosci. 114 G00F02.

1151 LaSage, D.M., Sexton, J.L., Mukherjee, A., Fryar, A.E., Greb, S.F., 2008. Groundwater discharge along
1152 a channelized Coastal Plain stream. J. Hydrol. 360 (1) 252–264.

1153 Laturnus, F., Haselmann, K.F., Borch, T., Grøn, C., 2002. Terrestrial natural sources of trichloromethane
1154 (chloroform, CHCl3)–an overview. Biogeochemistry 60 (2) 121−139.

1155 Lautz, L.K., Fanelli, R.M., 2008. Seasonal biogeochemical hotspots in the streambed around restoration
1156 structures. Biogeochem. 91 (1) 85–104.

1157 Lawrence, J.E., Skold, M.E., Hussain, F.A., Silverman, D.R., Resh, V.H., Sedlak, D.L., Luthy, R.G.,
1158 McCray, J.E., 2013. Hyporheic zone in urban streams: a review and opportunities for enhancing water
1159 quality and improving aquatic habitat by active management. Environ. Eng. Sci. 30 (8) 480–501.

1160 Le, N.B., Coleman, N.V., 2011. Biodegradation of vinyl chloride, cis-dichloroethene and 1, 2-
1161 dichloroethane in the alkene/alkane-oxidising *Mycobacterium* strain NBB4. Biodegradation, 22 (6)
1162 1095–1108.

1163 Lee, I.S., Bae, J.H., McCarty, P.L., 2007. Comparison between acetate and hydrogen as electron donors
1164 and implications for the reductive dehalogenation of PCE and TCE. J. Cont. Hydrol. 94 (1) 76−85.

1165 Lee, M., Low, A., Zemb, O., Koenig, J., Michaelsen, A., Manefield, M., 2012. Complete chloroform
1166 dechlorination by organochlorine respiration and fermentation. Environ. Microbiol. 14 (4) 883−894.

1167 Lewandowski, J., Nützmann, G., 2010. Nutrient retention and release in a floodplain's aquifer and in the
1168 hyporheic zone of a lowland river. Ecol. Eng. 36 (9) 1156–1166.

1169 Lewandowski, J., Rüter, K., Hupfer, M., 2002. Two-dimensional small-scale variability of pore water
1170 phosphate in freshwater lakes: results from a novel dialysis sampler. Environ. Sci. Technol. 36 (9) 2039–
1171 2047.

1172 Leys, D., Adrian, L., Smidt, H., 2013. Organohalide respiration: microbes breathing chlorinated
1173 molecules. Phil. Trans. R. Soc. B 368: 20120316.

1174 Liu, H., Chen, T., Frost, R.L., 2014. An overview of the role of goethite surfaces in the environment.
1175 Chemosphere 103 1−11.

1176 Löffler, F.E., Sanford, R.A., 2005. Analysis of trace hydrogen metabolism. Methods Enzymol. 397 222–
1177 237.

1178 Löffler, F.E., Sun, Q., Li, J., Tiedje, J.M., 2000. 16S rRNA gene-based detection of tetrachloroethene-
1179 dechlorinating *Desulfuromonas* and *Dehalococcoides* species. Appl. Environ. Microbiol. 66 (4)
1180 1369−1374.

1181 Löffler, F.E., Tiedje, J.M., Sanford, R.A., 1999. Fraction of electrons consumed in electron acceptor
1182 reduction and hydrogen thresholds as indicators of halorespiratory physiology. Appl. Environ.
1183 Microbiol. 65 (9) 4049–4056.

1184 Löffler, F.E., Yan, J., Ritalahti, K.M., Adrian, L., Edwards, E.A., Konstantinidis, K.T., Müller, J.A.,
1185 Fullerton, H., Zinder, S.H., Spormann, A.M., 2013. *Dehalococcoides mccartyi* gen. nov., sp. nov.,
1186 obligately organohalide-respiring anaerobic bacteria relevant to halogen cycling and bioremediation,
1187 belong to a novel bacterial class, *Dehalococcoidia* classis nov., order *Dehalococcoidales* ord. nov. and
1188 family *Dehalococcoidaceae* fam. nov., within the phylum *Chloroflexi*. Int. J. Syst. Evol. Microbiol. 63
1189 (2) 625−635.

1190 Lorah, M.M., Dyer, L.J., Burris, D.R., 2007. Anaerobic biodegradation and hydrogeochemical controls
1191 on natural attenuation of trichloroethene in an inland forested wetland. Bioremed. J. 11 (2) 85−102.

1192 Lorah, M.M., Olsen, L.D., 1999. Natural attenuation of chlorinated volatile organic compounds in a
1193 freshwater tidal wetland: Field evidence of anaerobic biodegradation. Water Res. Res. 35 (12) 3811–
1194 3827.

1195 Lovely, D.R., Goodwin, S., 1988. Hydrogen concentrations as an indicator of the predominant
1196 terminal electron accepting process in aquatic sediments. Geochim. Cosmochim. Acta 52 11–18.

1197 Lovley, D. R., 1985, Minimum threshold for hydrogen metabolism in methanogenic bacteria. Appl.
1198 Environ. Microbiol. 49 (6) 1530–1531.

1199 Lovley, D.R., Phillips, E.J.P., Lonergan, D. J., 1989. Hydrogen and formate oxidation coupled to
1200 dissimilatory reduction of iron or manganese by *Alteromonas putrefaciens*. Appl. Environ. Microbiol.
1201 55 700–706.

1202 Lu Y, Atashgahi, S., Hug L.A., Smidt H., 2015. Primers that target functional genes of organohalide-
1203 respiring bacteria. In: McGenity, T.J., Timmis, K.N., Nogales, B., (Eds.) Hydrocarbon and lipid
1204 microbiology protocols: methods to detect specific individuals and groups in communities. Springer
1205 Protocols Handbook. Springer-Verlag, Berlin, Heidelberg. pp. 177–205.

1206 Lu, Q., Luo, Q.S., Li, H., Di Liu, Y., Gu, J.D., Lin, K.F., 2015. Characterization of chlorinated aliphatic
1207 hydrocarbons and environmental variables in a shallow groundwater in Shanghai using kriging
1208 interpolation and multifactorial analysis. PloS one 10 (11), e0142241.

1209 Lu, X.X., Tao, S., Bosma, T., Gerritse, J., 2001. Characteristic hydrogen concentrations for various
1210 redox processes in batch study. J. Environ. Sci. Health Part A, 36 (9) 1725–1734.

1211 Lu, Y., Ramiro-Garcia, J., Vandermeeren, P., Herrmann, S., Cichocka, D., Springael, D., Atashgahi, S.,
1212 Smidt, H., 2017. Dechlorination of three tetrachlorobenzene isomers by contaminated harbor sludge-
1213 derived enrichment cultures follows thermodynamically favorable reactions. Appl. Microbiol. Biotech.
1214 101: 2589–2601.

1215 Luijten, M.L.G.C., Roelofsen, W., Langenhoff, A.A.M., Schraa, G., Stams, A.J. M., 2004. Hydrogen
1216 threshold concentrations in pure cultures of halorespiring bacteria and at a site polluted with chlorinated
1217 ethenes. Environ. Microbiol. 6 (6) 646–650.

1218 Mani, S., Sundaram, J., Das, K.C., 2016. Process simulation and modeling: Anaerobic digestion of
1219 complex organic matter. Biomass and Bioenerg. 93 58−167.

1220 Mao, X., Polasko, A., Alvarez-Cohen, L., 2017. Effects of sulfate reduction on trichloroethene
1221 dechlorination by *dehalococcoides*-containing microbial communities. Appl. Environ. Microbiol. 83 (8)
1222 e03384-16.

1223 Mattes, T.E., Alexander, A.K., Coleman, N.V., 2010. Aerobic biodegradation of the chloroethenes:
1224 pathways, enzymes, ecology, and evolution. FEMS Microbiol. Rev. 34 (4) 445−475.

1225 Mayer-Blackwell, K., Fincker, M., Molenda, O., Callahan, B., Sewell, H., Holmes, S., Edwards, E.A.,
1226 Spormann, A.M., 2016. 1, 2-Dichloroethane exposure alters the population structure, metabolism, and
1227 kinetics of a trichloroethene-dechlorinating *Dehalococcoides mccartyi* consortium. Environ. Sci.
1228 Technol. 50 (22) 12187−12196.

1229 Maymo-Gatell, X., Chien, Y.T., Gossett, J.M., Zinder, S.H., 1997. Isolation of a bacterium that
1230 reductively dechlorinates tetrachloroethene to ethene. Science 276 (5318) 1568−1571.

1231 Maymo-Gatell, X., Nijenhuis, I., Zinder, S.H., 2001. Reductive dechlorination of cis-1,2-dichloroethene
1232 and vinyl chloride by "*Dehalococcoides ethenogenes*". Environ. Sci. Technol. 35 516-−521.

1233 Mazur, C.S., Jones, W.J., 2001. Hydrogen concentrations in sulfate-reducing estuarine sediments during
1234 PCE dehalogenation. Environ. Sci. Technol. 35 4783−4788.

1235 McCarty, P.L., 1997. Breathing with chlorinated solvents. Science 276 (5318) 1521−1522.

1236 McGuire, T.M., Newell, C.J., Looney, B.B., Vangelas, K.M. and Sink, C.H., 2004. Historical analysis
1237 of monitored natural attenuation: A survey of 191 chlorinated solvent sites and 45 solvent plumes.
1238 Remed. J. 15 (1) 99–112.

1239 McKnight, U.S., Funder, S.G., Rasmussen, J.J., Finkel, M., Binning, P.J., Bjerg, P.L., 2010. An
1240 integrated model for assessing the risk of TCE groundwater contamination to human receptors and
1241 surface water ecosystems. Ecol. Eng. 36 1126−1137.

1242 McKnight, U.S., Rasmussen, J.J., Kronvang, B., Bjerg, P.L., Binning, P.J., 2012. Integrated assessment
1243 of the impact of chemical stressors on surface water ecosystems. Sci. Total Environ. 427 319–331.

1244 Meckenstock, R.U., Elsner, M., Griebler, C., Lueders, T., Stumpp, C., Aamand, J., Agathos, S.N.,
1245 Albrechtsen, H.J., Bastiaens, L., Bjerg, P.L., Boon, N., 2015. Biodegradation: updating the concepts of
1246 control for microbial cleanup in contaminated aquifers. Environ. Sci. Technol. 2015, 49, 7073−7081.

1247 Men, Y., Feil, H., VerBerkmoes, N.C., Shah, M.B., Johnson, D.R., Lee, P.K., West, K.A., Zinder, S.H.,
1248 Andersen, G.L., Alvarez-Cohen, L., 2012. Sustainable syntrophic growth of *Dehalococcoides*
1249 *ethenogenes* strain 195 with *Desulfovibrio vulgaris* Hildenborough and *Methanobacterium congolense*:
1250 global transcriptomic and proteomic analyses. ISME J. 6 (2) 410−421.

1251 Men, Y., Lee, P.K., Harding, K.C., Alvarez-Cohen, L., 2013. Characterization of four TCE-
1252 dechlorinating microbial enrichments grown with different cobalamin stress and methanogenic
1253 conditions. Appl. Microbiol. Biotechnol., 97 (14) 6439−6450.

1254 Mendoza-Lera, C., Frossard, A., Knie, M., Federlein, L.L., Gessner, M.O., Mutz, M., 2017. Importance
1255 of advective mass transfer and sediment surface area for streambed microbial communities. Freshwater
1256 Biol. 62 (1) 133–145.

1257 Menichino, G.T., Hester, E.T., 2015. The effect of macropores on bi-directional hydrologic exchange
1258 between a stream channel and riparian groundwater. J. Hydrol. 529 830–842.

1259 Mermillod-Blondin, F., Mauclaire, L., Montuelle, B., 2005. Use of slow filtration columns to assess
1260 oxygen respiration, consumption of dissolved organic carbon, nitrogen transformations, and microbial
1261 parameters in hyporheic sediments. Water Res. 39 (9) 1687–1698.

1262 Mermillod-Blondin, F., Winiarski, T., Foulquier, A., Perrissin, A., Marmonier, P., 2015. Links between
1263 sediment structures and ecological processes in the hyporheic zone: ground-penetrating radar as a
1264 non-invasive tool to detect subsurface biologically active zones. Ecohydrology 8 (4) 626–641.

1265 Meyer, J.L., Paul, M.J., Taulbee, W. K., 2005. Stream ecosystem function in urbanizing landscapes. J.
1266 N. Am. Benthol. Soc. 24, 602−612.

1267 Milosevic, N., Thomsen, N.I., Juhler, R.K., Albrechtsen, H.J., Bjerg, P.L., 2012. Identification of
1268 discharge zones and quantification of contaminant mass discharges into a local stream from a landfill in
1269 a heterogeneous geologic setting. J. Hydrol. 446 13–23.

1270 Mineau, M.M., Rigsby, C.M., Ely, D.T., Fernandez, I.J., Norton, S.A., Ohno, T., Valett, H., Simon,
1271 K.S., 2013. Chronic catchment nitrogen enrichment and stoichiometric constraints on the bioavailability
1272 of dissolved organic matter from leaf leachate. Freshwater Biol. 58 (2) 248–260.

1273 Mohn, W.W., Tiedje, J.M., 1992. Microbial reductive dehalogenation. Microbiol. Rev. 56 (3) 482− 507.

1274 Morris, B.E., Henneberger, R., Huber, H., Moissl-Eichinger, C., 2013. Microbial syntrophy: interaction
1275 for the common good. FEMS Microbiol. Rev. 37 (3) 384–406.

1276 Munz, M., Oswald, S.E., Schmidt, C., 2016. Analysis of riverbed temperatures to determine the
1277 geometry of subsurface water flow around in-stream geomorphological structures. J. Hydrol. 539 74–
1278 87.

1279 Naranjo, R.C., Niswonger, R.G., Davis, C.J., 2015. Mixing effects on nitrogen and oxygen
1280 concentrations and the relationship to mean residence time in a hyporheic zone of a riffle-pool sequence.
1281 Water Resour. Res. 51 (9), 7202–7217.

1282 Nath, K., Das, D., 2004. Improvement of fermentative hydrogen production: various approaches. Appl.
1283 Microbiol. Biotechnol. 65 (5) 520–529.

1284 Navel, S., Sauvage, S., Delmotte, S., Gerino, M., Marmonier, P., Mermillod-Blondin, F., 2012. A
1285 modelling approach to quantify the influence of fine sediment deposition on biogeochemical processes
1286 occurring in the hyporheic zone. Ann. Limnol. - Int. J. Lim. 48 279–287.

1287 Nelson, D.K., Hozalski, R.M., Clapp, L.W., Semmens, M.J., Novak, P.J., 2002. Effect of nitrate and
1288 sulfate on dechlorination by a mixed hydrogen-fed culture. Bioremed. J. 6 (3) 225−236.

1289 Ng, D.H., Kumar, A., Cao, B., 2016. Microorganisms meet solid minerals: interactions and
1290 biotechnological applications. Appl. Microbiol. Biotechnol. 100 (16) 6935−6946.

1291 Nogaro, G., Datry, T., Mermillod-Blondin, F., Foulquier, A., Montuelle, B., 2013. Influence of
1292 hyporheic zone characteristics on the structure and activity of microbial assemblages. Freshwater Biol.
1293 58 (12) 2567–2583.

1294 Nogaro, G., Mermillod-Blondin, F., Montuelle, B., Boisson, J.C., Bedell, J.P., Ohannessian, A., Volat,
1295 B., Gibert, J., 2007. Influence of a stormwater sediment deposit on microbial and biogeochemical
1296 processes in infiltration porous media. Sci. Total Environ. 377 (2) 334–348.

1297 Nyquist, J.E., Freyer, P.A., Toran, L., 2008. Stream bottom resistivity tomography to map ground water
1298 discharge. Ground water, 46 (4) 561–569.

1299 Oldenhuis, R., Oedzes, J.Y., Van der Waarde, J.J., Janssen, D.B., 1991. Kinetics of chlorinated
1300 hydrocarbon degradation by Methylosinus trichosporium OB3b and toxicity of trichloroethylene. Appl.
1301 Environ. Microbiol. 57 (1) 7–14.

1302 Oldham, C.E., Farrow, D.E., Peiffer, S., 2013. A generalized Damkohler number for classifying material
1303 processing in hydrological systems. Hydrol. Earth Sys. Sci. Discuss. 17 (3) 1133.

1304 Paes, F., Liu, X., Mattes, T. E., Cupples, A. M., 2015. Elucidating carbon uptake from vinyl chloride
1305 using stable isotope probing and Illumina sequencing. Appl. Microbiol. Biotechnol. 99 (18) 7735−7743.

1306 Palmer-Felgate, E.J., Mortimer, R.J., Krom, M.D., Jarvie, H.P., 2010. Impact of point-source pollution
1307 on phosphorus and nitrogen cycling in stream-bed sediments. Environ. Sci. Technol. 44 (3) 908–914.

1308 Pankow, J.F., Cherry, J.A., 1996. Dense chlorinated solvents and other DNAPLs in groundwater:
1309 History, behavior, and remediation. Waterloo Press, University of Waterloo.

1310 Pantazidou, M., Panagiotakis, I., Mamais, D. and Zikidi, V., 2012. Chloroethene biotransformation in
1311 the presence of different sulfate concentrations. Groundwater Monit. Remediat. 32 (1) 106−119.

1312 Parker, B.L., Gillham, R.W., Cherry, J.A., 1994. Diffusive disappearance of immiscible-phase organic
1313 liquids in fractured geologic media. Ground Water 32 (5) 805–820.

1314 Paul, L., Herrmann, S., Koch, C.B., Philips, J., Smolders, E., 2013. Inhibition of microbial
1315 trichloroethylene dechorination by Fe (III) reduction depends on Fe mineralogy: A batch study using
1316 the bioaugmentation culture KB-1. Water Res. 47 (7) 2543−2554.

1317 Paul, L., Jakobsen, R., Smolders, E., Albrechtsen, H.J., Bjerg, P.L., 2016. Reductive dechlorination of
1318 trichloroethylene (TCE) in competition with Fe and Mn oxides−Observed dynamics in H_2-dependent
1319 terminal electron accepting processes. Geomicrobiol. J. 33 (5) 357−366.

1320 Pavlostathis, S.G., Zhuang, P., 1993. Reductive dechlorination of chloroalkenes in microcosms
1321 developed with a field contaminated soil. Chemosphere 27 (4) 585−595.

1322 Peng, S.B., Huang, J.L., Zhong, X.H., Yang, J.C., Wang, G.H., Zou, Y.B., Zhang, F.S., Zhu, Q.S.,
1323 Buresh, R., Witt, C., 2002. Challenge and opportunity in improving fertilizer-nitrogen use efficiency of
1324 irrigated rice in China. Agr. Sci. China 1 (7) 776−785.

1325 Pérez-de-Mora, A., Zila, A., McMaster, M.L., Edwards, E.A., 2014. Bioremediation of chlorinated
1326 ethenes in fractured bedrock and associated changes in dechlorinating and nondechlorinating microbial
1327 populations. Environ. Sci. Technol. 48 (10) 5770−5779.

1328 Pinay, G., Peiffer, S., De Dreuzy, J.R., Krause, S., Hannah, D.M., Fleckenstein, J.H., Sebilo, M., Bishop,
1329 K., Hubert-Moy, L., 2015. Upscaling nitrogen removal capacity from local hotspots to low stream
1330 orders' drainage basins. Ecosystems 18 (6) 1101–1120.

1331 Pitkin, S.E., Cherry, J.A., Ingelton, R.A., Broholm, M., 1999. Field demonstrations using the Waterloo
1332 groundwater profiler. Ground Water Monit. Remediat. 19 (2) 122–131

1333 Puigserver, D., Cortés, A., Viladevall, M., Nogueras, X., Parker, B.L., Carmona, J.M., 2014. Processes
1334 controlling the fate of chloroethenes emanating from DNAPL aged sources in river–aquifer contexts. J.
1335 Cont. Hydrol. 168 25−40.

1336 Pusch, M., Schwoerbel, J., 1994. Community respiration in hyporheic sediments of a mountain stream
1337 (Steina, Black Forest). Archiv für Hydrobiologie 130 (1) 35−52.

1338 Rahimi, M., Essaid, H.I., Wilson, J.T., 2015. The role of dynamic surface water-groundwater exchange
1339 on streambed denitrification in a first-order, low-relief agricultural watershed. Water Resour. Res. 51
1340 (12) 9514–9538.

1341 Rasche, M.E., Hyman, M.R., Arp, D.J., 1991. Factors limiting aliphatic chlorocarbon degradation by
1342 Nitrosomonas europaea: cometabolic inactivation of ammonia monooxygenase and substrate
1343 specificity. Appl. Environ. Microbiol. 57 (10) 2986–2994.

1344 Rasmussen, J.J., McKnight, U.S., Sonne, A.T., Wiberg-Larsen, P., Bjerg, P.L., 2016. Legacy of a
1345 Chemical Factory Site: Contaminated Groundwater Impacts Stream Macroinvertebrates. Arch. Environ.
1346 Contam. Toxicol. 70 (2) 219–230.

1347 Ribot, M., Von Schiller, D., Peipoch, M., Sabater, F., Grimm, N.B., Martí, E., 2013. Influence of nitrate
1348 and ammonium availability on uptake kinetics of stream biofilms. Freshwater Sci. 32 (4) 1155–1167.

1349 Richardson, R.E., 2016. Organohalide-Respiring Bacteria as Members of Microbial Communities:
1350 Catabolic Food Webs and Biochemical Interactions. In: Lorenz., A., Löffler, F., (Eds.) Organohalide-
1351 Respiring Bacteria. Springer Berlin, Heidelberg, pp. 309−341.

1352 Rinehart, A.J., Jones Jr, J.B., Harms, T.K., 2015. Hydrologic and biogeochemical influences on carbon
1353 processing in the riparian zone of a subarctic stream. Freshwater Sci. 34 (1) 222−232.

1354 Rivett, M.O., Buss, S.R., Morgan, P., Smith, J.W., Bemment, C.D., 2008a. Nitrate attenuation in
1355 groundwater: a review of biogeochemical controlling processes. Water Res. 42 (16) 4215−4232.

1356 Rivett, M.O., Dearden, R.A., Wealthall, G.P., 2014. Architecture, persistence and dissolution of a 20 to
1357 45year old trichloroethene DNAPL source zone. J. Contam. Hydrol. 170, 95–115.

1358 Rivett, M.O., Ellis, P.A., Greswell, R.B., Ward, R.S., Roche, R.S., Cleverly, M.G., Walker, C., Conran,
1359 D., Fitzgerald, P.J., Willcox, T. Dowle, J., 2008b. Cost-effective mini drive-point piezometers and
1360 multilevel samplers for monitoring the hyporheic zone. Q. J. Eng. Geol. Hydr. 41 (1) 49–60.

1361 Rivett, M.O., Feenstra, S., 2005. Dissolution of an emplaced source of DNAPL in a natural aquifer
1362 setting. Environ. Sci. Technol. 39 (2) 447–455.

1363 Rivett, M.O., Feenstra, S., Clark, L., 2006. Lyne and McLachlan (1949): influence of the first
1364 publication on groundwater contamination by trichloroethene. Environ. Forensics 7 (4), 313–323.

1365 Rivett, M.O., Turner, R.J., Glibbery, P., Cuthbert, M.O., 2012. The legacy of chlorinated solvents in the
1366 Birmingham aquifer, UK: Observations spanning three decades and the challenge of future urban
1367 groundwater development. J. Contam. Hydrol. 140, 107–123.

1368 Roche R.S., Rivett M.O., Tellam J.H., Cleverly M.G., Walker M., 2008. Natural attenuation of a TCE
1369 plume at the groundwater–surface-water interface: spatial and temporal variability within a 50 m reach.
1370 GQ07: securing groundwater quality in urban and industrial environments. IAHS Publ., pp. 475–82.

1371 Romaní, A.M., Vázquez, E., Butturini, A., 2006. Microbial availability and size fractionation of
1372 dissolved organic carbon after drought in an intermittent stream: biogeochemical link across the stream–
1373 riparian interface. Microb. Ecol. 52 (3) 501–512.

1374 Rønde, V., McKnight, U.S., Sonne, A.T., Balbarini, N., Devlin, J.F., Bjerg, P.L., 2017. Contaminant
1375 mass discharge to streams: Comparing direct groundwater velocity measurements and multi-level
1376 groundwater sampling with an in-stream approach. J. Cont. Hydrol. DOI:
1377 10.1016/j.jconhyd.2017.09.010

1378 Rosenberry, D.O., Briggs, M.A., Delin, G., Hare, D.K., 2016. Combined use of thermal methods and
1379 seepage meters to efficiently locate, quantify, and monitor focused groundwater discharge to a sand-bed
1380 stream. Water Resour. Res. 52 (6) 4486–4503.

1381 Rowe, B.L., Toccalino, P.L., Moran, M.J., Zogorski, J.S., Price, C.V., 2007. Occurrence and potential
1382 human–health relevance of volatile organic compounds in drinking water from domestic wells in the
1383 United States. Environ. Health Perspect. 115 (11) 1539.

1384 Roy, J.W., Bickerton, G., 2010. Proactive screening approach for detecting groundwater contaminants
1385 along urban streams at the reach-scale. Environ. Sci. Technol. 44 (16) 6088–6094.

1386 Roy, J.W., Bickerton, G., 2011. Toxic groundwater contaminants: an overlooked contributor to urban
1387 stream syndrome? Environ. Sci. Technol. 46 (2) 729–736.

1388 Roy, J.W., Grapentine, L., Bickerton, G., 2017. Ecological effects from groundwater contaminated by
1389 volatile organic compounds on an urban stream's benthic ecosystem. Limnologica–Ecology and
1390 Management of Inland Waters. DOI:10.1016/j.limno.2017.01.004.

1391 Rulík, M., Čáp, L. and Hlaváčová, E., 2000. Methane in the hyporheic zone of a small lowland stream
1392 (Sitka, Czech Republic). Limnologica - Ecology and Management of Inland Waters 30 (4) 359−366.

1393 Rulik, M., Hekera, P., 1998. Occurence of both acetic and lactic acids in subsurface water of the bed
1394 sediments: comparison of two different localities. In: Bretschko, G., Helešivic, J. (Eds.) Advances in
1395 River Bottom Ecology. Backhuys Publishers, Leiden pp. 77−87.

1396 Ryoo, D., Shim, H., Canada, K., Barbieri, P., Wood, T.K., 2000. Aerobic degradation of
1397 tetrachloroethylene by toluene-o-xylene monooxygenase of Pseudomonas stutzeri OX1. Nat.
1398 Biotechnol. 18 (7) 775–778.

1399 Sanders, I.A., Heppell, C.M., Cotton, J.A., Wharton, G., Hildrew, A.G., Flowers, E.J., Trimmer, M.,
1400 2007. Emission of methane from chalk streams has potential implications for agricultural practices.
1401 Freshwater Biol. 52 (6) 1176−1186.

1402 Sawyer, A.H., Cardenas, M.B., 2009. Hyporheic flow and residence time distributions in heterogeneous
1403 cross-bedded sediment. Water Resour. Res. 45 (8) W08406.

1404 Scheutz, C., Durant, N.D., Hansen, M.H., Bjerg, P.L., 2011. Natural and enhanced anaerobic
1405 degradation of 1,1,1-trichloroethane and its degradation products in the subsurface–a critical review.
1406 Water Res. 45 (9) 2701−2723.

1407 Schmidt, C., Bayer-Raich, M., Schirmer, M., 2006. Characterization of spatial heterogeneity of
1408 groundwater-stream water interactions using multiple depth streambed temperature measurements at the
1409 reach scale. Hydrol. Earth Sys. Sci. Discuss. 3 (4) 1419–1446.

1410 Schmidt, C., Conant, B., Bayer-Raich, M., Schirmer, M., 2007. Evaluation and field-scale application
1411 of an analytical method to quantify groundwater discharge using mapped streambed temperatures. J.
1412 Hydrol. 347 (3) 292–307.

1413 Schmidt, K.R., Augenstein, T., Heidinger, M., Ertl, S., Tiehm, A., 2010. Aerobic biodegradation of cis-
1414 1,2-dichloroethene as sole carbon source: stable carbon isotope fractionation and growth characteristics.
1415 Chemosphere, 78 (5) 527−532.

1416 Schmidt, K.R., Gaza, S., Voropaev, A., Ertl, S., Tiehm, A., 2014. Aerobic biodegradation of
1417 trichloroethene without auxiliary substrates. Water Res. 59 112−118.

1418 Sela-Adler, M., Ronen, Z., Herut, B., Antler, G., Vigderovich, H., Eckert, W., Sivan, O., 2017. Co-
1419 existence of methanogenesis and sulfate reduction with common substrates in sulfate-rich estuarine
1420 sediments. Front. Microbiol. DOI: 10.3389/fmicb.2017.00766.

1421 Semprini, L., Hopkins, G.D., McCarty, P.L., 1994. A field and modeling comparison of in situ
1422 transformation of trichloroethylene by methane utilizers and phenol utilizers. Lewis Publishers, Boca
1423 Raton, pp. 284–254.

1424 Seyedabbasi, M.A., Newell, C.J., Adamson, D.T., Sale, T.C., 2012. Relative contribution of DNAPL
1425 dissolution and matrix diffusion to the long-term persistence of chlorinated solvent source zones. J.
1426 Contam. Hydrol. 134 69–81.

1427 Sharma, P.K., McCarty, P.L., 1996. Isolation and characterization of a facultatively aerobic bacterium
1428 that reductively dehalogenates tetrachloroethene to cis-1,2-dichloroethene. Applied and Environ.
1429 Microbiol. 62 (3) 761−765.

1430 Shelley, F., Abdullahi, F., Grey, J., Trimmer, M., 2015. Microbial methane cycling in the bed of a chalk
1431 river: oxidation has the potential to match methanogenesis enhanced by warming. Freshwater Biol. 60
1432 (1) 150−160.

1433 Shim, H., Ryoo, D., Barbieri, P., Wood, T.K., 2001. Aerobic degradation of mixtures of
1434 tetrachloroethylene, trichloroethylene, dichloroethylenes, and vinyl chloride by toluene-o-xylene
1435 monooxygenase of *Pseudomonas stutzeri* OX1. Appl. Microbiol. Biotechnol. 56 (1) 265–269.

1436 Sieber, J.R., Le, H.M., McInerney, M.J., 2014. The importance of hydrogen and formate transfer for
1437 syntrophic fatty, aromatic and alicyclic metabolism. Environ. Microbiol. 16 (1) 177–188.

1438 Sieber, J.R., Sims, D.R., Han, C., Kim, E., Lykidis, A., Lapidus, A.L., McDonnald, E., Rohlin, L.,
1439 Culley, D.E., Gunsalus, R., McInerney, M.J., 2010. The genome of Syntrophomonas wolfei: new
1440 insights into syntrophic metabolism and biohydrogen production. Environ. Microbiol. 12 (8), 2289–
1441 2301.

1442 Simsir, B., Yan, J., Im, J., Graves, D., Löffler, F.E., 2017. Natural attenuation in streambed sediment
1443 receiving chlorinated solvents from underlying fracture networks. Environ. Sci. Technol. 51 (9) 4821–
1444 4830.

1445 Smidt, H., de Vos, W.M., 2004. Anaerobic microbial dehalogenation. Ann. Rev. Microbiol. 58 43−73.

1446 Sobczak, W.V., Findlay, S., 2002. Variation in bioavailability of dissolved organic carbon among stream
1447 hyporheic flowpaths. Ecology 83 (11) 3194–3209.

1448 Sonne, A.T., McKnight, U. S., Rønde, V., Bjerg, P.L., 2017. Assessing the chemical contamination
1449 dynamics in a mixed land use stream system. Water Research DOI: 10.1016./j.watres.2017.08.031.

1450 Squillace, P.J., Moran, M.J., 2007. Factors associated with sources, transport, and fate of volatile organic
1451 compounds and their mixtures in aquifers of the United States. Environ. Sci. Technol. 41 (7) 2123–
1452 2130.

1453 Stegen, J.C., Fredrickson, J.K., Wilkins, M.J., Konopka, A.E., Nelson, W.C., Arntzen, E.V., Chrisler,
1454 W.B., Chu, R.K., Danczak, R.E., Fansler, S.J., Kennedy, D.W., 2016. Groundwater-surface water
1455 mixing shifts ecological assembly processes and stimulates organic carbon turnover. Nat. Commun. 7:
1456 11237.

1457 Stelzer, R.S., Scott, J.T., Bartsch, L.A., Parr, T.B., 2014. Particulate organic matter quality influences
1458 nitrate retention and denitrification in stream sediments: evidence from a carbon burial experiment.
1459 Biogeochemistry 119 (1-3) 387−402.

1460 Storey, R.G., Fulthorpe, R.R., Williams, D.D., 1999. Perspectives and predictions on the microbial
1461 ecology of the hyporheic zone. Freshwater Biol. 41 (1), 119–130.

1462 Sung, Y., Fletcher, K.E., Ritalahti, K.M., Apkarian, R.P., Ramos-Hernández, N., Sanford, R.A.,
1463 Mesbah, N.M., Löffler, F.E., 2006. *Geobacter lovleyi* sp. nov. strain SZ, a novel metal-reducing and
1464 tetrachloroethene-dechlorinating bacterium. Appl. Environ. Microbiol. 72 (4) 2775−2782.

1465 Suttinun, O., Luepromchai, E., Müller, R., 2013. Cometabolism of trichloroethylene: concepts,
1466 limitations and available strategies for sustained biodegradation. Rev. Environ. Sci. Biotechnol. 12 (1)
1467 99–114.

1468 Sutton, N.B., Atashgahi, S., Saccenti, E., Grotenhuis, T., Smidt, H., Rijnaarts, H.H.M., 2015. Microbial
1469 community response of an organohalide respiring enrichment culture to permanganate oxidation. PLoS
1470 One 10: e0134615.

1471 Tan, K., Anderson, T.A., Jackson, W.A., 2005. Temporal and spatial variation of perchlorate in
1472 streambed sediments: results from in-situ dialysis samplers. Environ. Pollut. 136 (2) 283–291.

1473 Taş, N., van Eekert, M.H., Wagner, A., Schraa, G., de Vos, W.M., Smidt, H., 2011. Role of
1474 "Dehalococcoides" spp. in the anaerobic transformation of hexachlorobenzene in European rivers. Appl.
1475 Environ. Microbiol. 77 (13) 4437−4445.

1476 Ter Meer, J., Gerritse, J., Di Mauro, C., Harkes, M.P., Rijnaarts, H.H.M., Cinjee, A.C., van Liere, I.H.,
1477 Slenders, I.H., Baartmans, R.F.W., 1999. Hydrogen as indicator for in-situ redox condition and
1478 dechlorination. Natural Attenuation of Environmental Contaminants, TNO-MEP R 99/341. TNO
1479 Institute of Environmental Sciences, Energy Research and Process Innovation, The Netherlands, pp.1-
1480 125.

1481 Tiehm, A., Schmidt, K.R., 2011. Sequential anaerobic/aerobic biodegradation of chloroethenes—
1482 aspects of field application. Curr. Opin. Biotechnol. 22 (3) 415−421.

1483 Tiehm, A., Schmidt, K.R., Pfeifer, B., Heidinger, M., Ertl, S., 2008. Growth kinetics and stable carbon
1484 isotope fractionation during aerobic degradation of cis-1, 2-dichloroethene and vinyl chloride. Water
1485 Res. 42 (10) 2431−2438.

1486 Trauth, N., Schmidt, C., Vieweg, M., Maier, U., Fleckenstein, J.H., 2014. Hyporheic transport and
1487 biogeochemical reactions in pool-riffle systems under varying ambient groundwater flow conditions. J.
1488 Geophys. Res. Biogeosci. 119 (5) 910–928.

1489 Trauth, N., Schmidt, C., Vieweg, M., Oswald, S.E., Fleckenstein, J.H., 2015. Hydraulic controls of
1490 in-stream gravel bar hyporheic exchange and reactions. Water Resour. Res. 51 (4) 2243−2263.

1491 Trimmer, M., Maanoja, S., Hildrew, A.G., Pretty, J.L., Grey, J., 2010. Potential carbon fixation via
1492 methane oxidation in well-oxygenated riverbed gravels. Limnol. Oceanogr. 55 (2) 560.

1493 Tristram, D.A., Krause, S., Levy, A., Robinson, Z.P., Waller, R.I., Weatherill, J.J., 2014. Identifying
1494 spatial and temporal dynamics of proglacial groundwater–surface-water exchange using combined
1495 temperature-tracing methods. Freshwater Sci. 34 (1) 99–110.

1496 Ullah, S., Zhang, H., Heathwaite, A.L., Binley, A., Lansdown, K., Heppell, K., Trimmer, M., 2012. In
1497 situ measurement of redox sensitive solutes at high spatial resolution in a riverbed using diffusive
1498 equilibrium in thin films (DET). Ecol. Eng. 49 18–26.

1499 Ullah, S., Zhang, H., Heathwaite, A.L., Heppell, C., Lansdown, K., Binley, A., Trimmer, M., 2014.
1500 Influence of emergent vegetation on nitrate cycling in sediments of a groundwater-fed river.
1501 Biogeochemistry 118 (1-3) 121−134.

1502 Vandermeeren, P., Herrmann, S., Cichocka, D., Busschaert, P., Lievens, B., Richnow, H.H., Springael,
1503 D., 2014. Diversity of dechlorination pathways and organohalide respiring bacteria in chlorobenzene
1504 dechlorinating enrichment cultures originating from river sludge. Biodegradation 25 (5) 757–776.

1505 Vannelli, T.O.D.D., Logan, M.Y.K.E., Arciero, D.M., Hooper, A.B., 1990. Degradation of halogenated
1506 aliphatic compounds by the ammonia-oxidizing bacterium *Nitrosomonas europaea*. Appl. Environ.
1507 Microbiol. 56 (4) 1169–1171.

1508 Verce, M.F., Ulrich, R.L., Freedman, D.L., 2000. Characterization of an isolate that uses vinyl chloride
1509 as a growth substrate under aerobic conditions. Appl. Environ. Microbiol. 66 (8) 3535−3542.

1510 Verce, M.F., Ulrich, R.L., Freedman, D.L., 2001. Transition from cometabolic to growth-linked
1511 biodegradation of vinyl chloride by a *Pseudomonas* sp. isolated on ethene. Environ. Sci. Technol. 35
1512 (21) 4242−4251.

1513 Vidon, P.G., Hill, A.R., 2004. Landscape controls on nitrate removal in stream riparian zones. Water
1514 Resour. Res. 40 (3) W03201.

1515 Vieweg, M., Kurz, M.J., Trauth, N., Fleckenstein, J.H., Musolff, A., Schmidt, C., 2016. Estimating
1516 time-variable aerobic respiration in the streambed by combining electrical conductivity and dissolved
1517 oxygen time series. J. Geophys. Res. Biogeosci. 121 (8) 2199−2215.

1518 Vogel, T.M., Criddle, C.S., McCarty, P.L., 1987. Transformation of halogenated aliphatic compounds.
1519 Environ. Sci. Technol. 21 (8) 722−736.

1520 Voisin, J., Cournoyer, B., Mermillod-Blondin, F., 2016. Assessment of artificial substrates for
1521 evaluating groundwater microbial quality. Ecol. Indic. 71 577–586.

1522 Wackett, L.P., Gibson, D.T., 1988. Degradation of trichloroethylene by toluene dioxygenase in whole-
1523 cell studies with *Pseudomonas putida* F1. Appl. Environ. Microbiol. 54 (7) 1703–1708.

1524 Wagner, D.D., Hug, L.A., Hatt, J.K., Spitzmiller, M.R., Padilla-Crespo, E., Ritalahti, K.M., Edwards,
1525 E.A., Konstantinidis, K.T., Löffler, F.E., 2012. Genomic determinants of organohalide-respiration in
1526 *Geobacter lovleyi*, an unusual member of the *Geobacteraceae*. BMC Genomics 13 (1) 200.

1527 Walker, C.B., He, Z., Yang, Z.K., Ringbauer, J.A., He, Q., Zhou, J., Voordouw, G., Wall, J.D., Arkin,
1528 A.P., Hazen, T.C., Stolyar, S., 2009. The electron transfer system of syntrophically grown *Desulfovibrio*
1529 *vulgaris*. J. Bacteriol. 191 (18) 5793–5801.

1530 Wang, G., Allen-King, R.M., Choung, S., Feenstra, S., Watson, R., Kominek, M., 2013. A practical
1531 measurement strategy to estimate nonlinear chlorinated solvent sorption in low foc sediments.
1532 Groundwater Monit. Remediat. 33 (1) 87 – 96.

1533 Weatherill, J. J., 2015. Investigating the natural attenuation and fate of a trichloroethene plume at the
1534 groundwater-surface water interface of a UK lowland river. PhD thesis, School of Physical and
1535 Geographical Sciences, Keele University, UK.

1536 Weatherill, J., Krause, S., Voyce, K., Drijfhout, F., Levy, A., Cassidy, N., 2014. Nested monitoring
1537 approaches to delineate groundwater trichloroethene discharge to a UK lowland stream at multiple
1538 spatial scales. J. Contam. Hydrol. 158 38–54.

1539 Wei, N., Finneran, K.T., 2011. Influence of ferric iron on complete dechlorination of trichloroethylene
1540 (TCE) to ethene: Fe (III) reduction does not always inhibit complete dechlorination. Environ. Sci.
1541 Technol. 45 (17) 7422−7430.

1542 Wei, N., Finneran, K.T., 2013. Low and high acetate amendments are equally as effective at promoting
1543 complete dechlorination of trichloroethylene (TCE). Biodegradation 24 (3) 413−425.

1544 Wiedemeier, T.D.H., Swanson, M.A., Moutoux,D.E., Gordon,K., Wilson, J.T., Wilson, B.H., Kampbell,
1545 D.H., Haas, P.E., Miller, R.N., Hansen, J.E., Chapelle, F.H., 1998. Technical Protocol for Evaluating
1546 Natural Attenuation of Chlorinated Solvents in Ground Water, IAG: RW57936164. US Environmental
1547 Protection Agency, USA.

1548 Wilson, F. P., Liu, X., Mattes, T. E., Cupples, A. M., 2016. *Nocardioides*, *Sediminibacterium*,
1549 *Aquabacterium*, *Variovorax*, and *Pseudomonas* linked to carbon uptake during aerobic vinyl chloride
1550 biodegradation. Environ. Sci. Pollut. Res. 23 (19) 19062−19070.

1551 Wittlingerová, Z., Macháčková, J., Petruželková, A., Zimová, M., 2016. Occurrence of
1552 perchloroethylene in surface water and fish in a river ecosystem affected by groundwater contamination.
1553 Environ. Sci. Pollut. Res. 23 (6) 5676–5692.

1554 Woessner, W.W., 2000. Stream and fluvial plain ground water interactions: rescaling hydrogeologic
1555 thought. Ground Water, 38 (3) 423–429.

1556 Wondzell, S.M., 2011. The role of the hyporheic zone across stream networks. Hydrol. Process. 25 (22)
1557 3525–3532.

1558 Wu, H., Chen, X.P., Liu, G.P., Jiang, M., Guo, T., Jin, W.Q., Wei, P., Zhu, D.W., 2012. Acetone–
1559 butanol–ethanol (ABE) fermentation using *Clostridium acetobutylicum* XY16 and in situ recovery by
1560 PDMS/ceramic composite membrane. Bioprocess Biosyst. Eng. 35 (7) 1057–1065.

1561 Yager, R.M., Bilotta, S.E., Mann, C.L., Madsen, E.L., 1997. Metabolic adaptation and in situ attenuation
1562 of chlorinated ethenes by naturally occurring microorganisms in a fractured dolomite aquifer near
1563 Niagara Falls, New York. Environ. Sci. Technol. 31 (11) 3138−3147.

1564 Yang, M., Annable, M.D., Jawitz, J.W., 2014. Back diffusion from thin low permeability zones.
1565 Environ. Sci. Technol. 49 (1) 415–422.

1566 Yang, Y., Higgins, S.A., Yan, J., Şimşir, B., Chourey, K., Iyer, R., Hettich, R.L., Baldwin, B., Ogles,
1567 D.M., Löffler, F.E., 2017. Grape pomace compost harbors organohalide-respiring Dehalogenimonas
1568 species with novel reductive dehalogenase genes. ISME J. DOI:10.1038/ismej.2017.127.

1569 Yang, Y., McCarty, P.L., 1998. Competition for hydrogen within a chlorinated solvent dehalogenating
1570 anaerobic mixed culture. Environ. Sci. Technol. 32 (22) 3591−3597.

1571 Yu, H.Y., Wang, Y.K., Chen, P.C., Li, F.B., Chen, M.J., Hu, M., Ouyang, X., 2014. Effect of nitrate
1572 addition on reductive transformation of pentachlorophenol in paddy soil in relation to iron (III)
1573 reduction. J. Environ. Manage. 132 42−48.

1574 Yu, S., Dolan, M.E., Semprini, L., 2005. Kinetics and inhibition of reductive dechlorination of
1575 chlorinated ethylenes by two different mixed cultures. Environ. Sci. Technol. 39 (1) 195−205.

1576 Yu, Z., Smith, G.B., 2000. Inhibition of methanogenesis by C1-and C2-polychlorinated aliphatic
1577 hydrocarbons. Environ. Toxicol. Chem. 19 (9) 2212−2217.

1578 Zarnetske, J.P., Haggerty, R., Wondzell, S.M., Baker, M.A., 2011. Labile dissolved organic carbon
1579 supply limits hyporheic denitrification. J. Geophys. Res. Biogeosci. 116 G04036.

1580 Zarnetske, J.P., Haggerty, R., Wondzell, S.M., Bokil, V.A., González-Pinzón, R., 2012. Coupled
1581 transport and reaction kinetics control the nitrate source-sink function of hyporheic zones. Water Resour.
1582 Res. 48 (11) W11508.

1583 Ziv-El, M., Popat, S.C., Cai, K., Halden, R.U., Krajmalnik-Brown, R., Rittmann, B.E., 2012. Managing
1584 methanogens and homoacetogens to promote reductive dechlorination of trichloroethene with direct
1585 delivery of H_2 in a membrane biofilm reactor. Biotechnol. Bioeng. 109 (9) 2200−2210.

1586 **Fig. 1.** Generic conceptual model of a groundwater CE plume discharging through heterogeneous
1587 hyporheic zone sediments with a range of solute residence times. The plume may be composed of HCEs,
1588 LCEs or a mixture of both. Dashed line indicates the approximate boundary between an upper oxic zone
1589 and lower suboxic/anoxic zone induced by buried sedimentary organic matter. OM: organic matter; K:
1590 sediment hydraulic conductivity. Brown areas in inset circles represents buried sedimentary organic
1591 matter (adapted from Gomez-Velez et al., 2014).

1592 **Fig. 2.** Schematic representation of hyporheic zone electron flow derived from complex organic matter
1593 metabolism (adapted from Heimann et al., 2009) to organohalide-respiring bacterial communities in
1594 anoxic riverbed sediments. Processes depicted include: orange arrow: hydrolysis; green arrows:
1595 fermentation; brown arrows: carbon assimilation; dashed red arrow: ammonification; dashed green
1596 arrow: methanogensis; blue arrows/lines: electron transport and red arrows: organohalide respiration.
1597 Ac: acetate; DIC: dissolved inorganic carbon; ETH: ethene. Representative Gibb's free energy (ΔG°)
1598 values (kJ/M) indicated for sequential reduction of PCE to ethene taken from Dolfing and Beurskens
1599 (1995) with representative Eh values from Wiedemeier et al. (1998) under standard conditions reported
1600 therein.

1601 **Fig. 3.** Influence of extracellular hydrogen concentrations on growth rates of fermenters and
1602 hydrogenotrophs (redrawn from Ter Meer et al., 1999).

1603 **Fig. 4.** Idealised ecological succession of terminal electron acceptors and their reduced metabolites in
1604 hyporheic zones based on observed molecular hydrogen (H_2) threshold concentrations. Ac: acetate;
1605 ETH: ethene. Gibb's free energy (ΔG°) values (kJ/M) from Heimann et al. (2009) with representative
1606 Eh values from Wiedemeier et al. (1998) under standard conditions reported therein. Observed minimum
1607 hydrogen threshold ranges: (1) Cord-Ruwish et al. (1988); (2) Haring et al. (1991); (3) Sung et al. (2006);
1608 (4) Lu et al. (2001); (5) Mazur et al. (2001); (6) Lovely et al. (1989); (7) Caccavo et al. (1992); (8)
1609 Luijten et al. (2004); (9) Lovely et al. (1985).

1610 **Fig. 5.** (a) Conceptual illustration of potential metabolic (black arrows) and co-metabolic mineralisation
1611 of cDCE and VC (red arrows) at the dispersive mixing zone between upwelling anoxic groundwater
1612 containing DOM by-products (ammonium and methane) and oxic hyporheic flow cells (blue arrows).

DIC: dissolved inorganic carbon; ETH: ethene. Note that reactive intermediates from co-metabolism are omitted for clarity. (b) Numerical simulations of oxygen concentration and uptake rate under gaining flow conditions in a dune bedform (adapted from Trauth et al., 2014). (c) Simulation of bedform mixing zone thickness with varying sediment hydraulic conductivity (K) and vertical groundwater flux (q_z) using a conservative groundwater tracer dilution approach (adapted from Hester et al., 2013).

Fig. 6. Vertical pore water chemical gradients from selected case studies illustrating a range of in-situ transformation capacities (refer to Table 1 for profile context and supporting information). Black diamonds: TCE; open squares: cDCE; open triangles: VC; green circles: ethane; blue circles: ethane; orange squares: methane. Redrawn from: (a) Weatherill et al. (2014); (b) Abe et al. (2009); (c) Freitas et al. (2015) and (d) Simsir et al. (2017).

Table 1: Field experience of chlorinated ethene plume discharging to surface water receptors illustrating a range of in-situ transformation potentials from selected case studies (continued overleaf).

Receptor	CE source	Aquifer	Plume	Mass flux to surface water (kg/y)	Residence time (d/m)	In-situ biotransformation potential	References
Grindsted Stream, Jutland, Denmark.	Pharmaceutical factory in operation from 1914 to 1999.	Quaternary and Tertiary sands, underlain by thick regional clay layer, natural gradients.	cDCE (47 µM) and VC (72 µM). Co-mingled hydrocarbons.	45–123 (cDCE), 42–123 (VC)	0.4–10	**Low**, although not specifically addressed. CE-impacted stream, also impacted by metals and other organic contaminants.	Rønde et al., 2017; Sonne et al., 2017.
Third Creek, Knoxville, Tenessee, USA.	Spills associated with historic metal processing facility operated for over a century.	Fractured/karstic dolomite. Overlain by silty-clay saprolite, natural gradients.	PCE and TCE (6-60 µM). Co-mingled 1,1,1-TCA, TCM, hydrocarbons.	16.1 (TCE + cDCE)	58	**High.** No CEs detectable in surface water. Stochiometric cDCE transformation in SO_4-reducing conditions and potential CH_4 cometabolism. Hydrocarbon co-contamiants source of SCFAs. Well distributed *D. mccartyi* population.	Simsir et al., 2017.
River Tame, Birmingham, UK.	Multiple historic urban/industrial sources, City of Birmingham.	Unconfined Permo-Triassic sandstones. Complex urban environment. Gradients historically affected by abstractions.	TCE + cDCE (0.25–9.5 µM). Measured in riverbed piezometers.	20–200 (TCE) over 7.4 km city reach	12–100 (sorption modified)	**Transiently high**, low-moderate overall. Stochiometric TCE transformation to ethene in riffle sequence under Mn(IV) reduction. HEF and buried SOM a source of DOC driving redox. Inhibition by high SO_4 (5 mM) suspected.	Freitas et al., 2015; Roche et al., 2009; Ellis and Rivett, 2007.

Zenne River, Vilvoorde, Belgium	Multiple industrial sources, Vilvoorde area.	Unconfined superficial gravel aquifer in urban setting. Gradients affected by retaining walls and canal water seepage.	VC (35 μM), cDCE (12 μM). 1.4 km wide plume.	Not addressed.	12–29	**High**. Transformation of cDCE and VC in up to 75% of locations. SOM-enriched sediments due to eutrophic conditions. *D. mccartyi* populations associated with SOM. VC/Ethene oxidisers present in SOM-poor zones.	Hamonts et al., 2009; 2012; Atashgahi et al., 2013; 2017a.
River Tern, Shropshire, UK.	Unknown. Suspected to be associated with a millitary airfield 1.5 km away.	Unconfined Permian sandstone. Natural gradients, occasional abstractions, agricultural setting.	TCE (0.1–1.4 μM).	0.15–0.55 (TCE)	0.5–1081 (sorption modified)	**Low** to **moderate** (patchy). Mass flux dominated by preferential pathways. Local TCE to cDCE hotspots associated peat lenses and surficial sediments. Elevated NO_3 in aerobic aquifer.	Weatherill et al., 2014; Weatherill, 2015.
Skensved Stream, Sjaelland, Denmark.	Leaking TCE storage tank, auto lacquer shop in operation since 1974. Leak discovered in 1993.	Interbedded soil, sand and gravel overlying bryozoan limestone. Pump-and-treat plume control in operation.	Max TCE (0.9 μM)	33 (TCE modelled from DNAPL source)	Not addressed	**Low,** aerobic to denitrifying conditions in hyporheic zone. Stream CE impact controlled by pump-and-treat system (as of 2009).	McKnight et al., 2010.
Pine River, Ontario, Canada.	Dry cleaning facility 195 m from river. PCE DNAPL contamination originated in the 1970s.	Semi-confined interbedded sand and clays in urban setting. Natural gradients.	Max PCE (0.25 mM)	3–53 (PCE) during 1995-1999.	858–71175 (sorption modified in silt/clay). Locally 3–23.	**High.** 52% of plume transformed to cDCE in riverbed. Stoichiometric ethene production in Fe(III)/SO_4 reducing SOM zones supporting *D. mccartyi* populations . Widespread aerobic VC mineralisation potential.	Conant et al., 2004; Abe et al., 2009.
Little Bayou Creek, McCracken County, Kentucky, USA.	Uranium enrichment facility, TCE used from 1953 to1996 for cleaning. Residual DNAPL volume of 795 m^3.	Regional gravel aquifer locally confined by silt and clay. Channelised river flow regime.	TCE near solubility limit near source (8.4 mM). 0.12–13 μM in riverbed. Co-mingled ^{99}Tc.	3-57 (TCE)	Not addressed	**Low**, TCE impacted surface water. No LCEs detectable in aerobic riverbed conditions with high mass flux through springs. Strong seasonal variability in stream water TCE concentrations.	LaSage et al., 2008; Fryar et al., 2000.

Unnamed Triburatary Streams, Industrial Facility, Conneticut, USA.	Manufacturing facility, 1970s underground degreaser tanks. TCE DNAPL source isolated in 1994. Plumes sustained by back-diffusion.	Unconfined surficial aquifer underlain by extensive aquitard. Steep topography, visible groundwater seepage zones.	TCE (18–24 μM), cDCE (5 μM) at Transect 2.	10 (TCE + cDCE) from Transect 2.	Not addressed	**Unknown.** Hyporheic zone processes in the streambeds not specifically investigated.	Chapman et al., 2007.

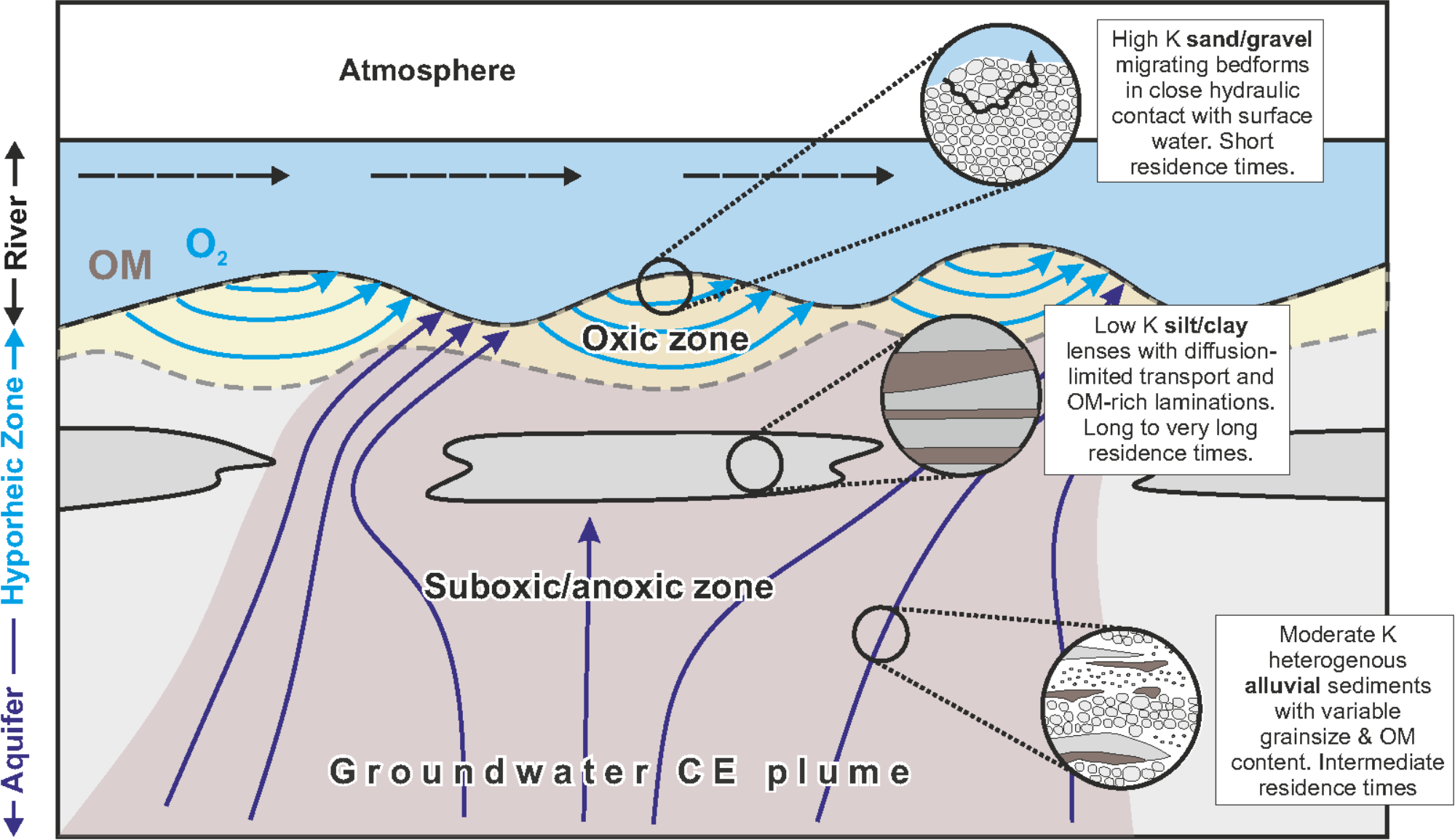
Atmosphere
High K **sand/gravel** migrating bedforms in close hydraulic contact with surface water. Short residence times.
OM
O_2
Oxic zone
Low K **silt/clay** lenses with diffusion-limited transport and OM-rich laminations. Long to very long residence times.
Suboxic/anoxic zone
Groundwater CE plume
Moderate K heterogenous **alluvial** sediments with variable grainsize & OM content. Intermediate residence times
River
Hyporheic Zone
Aquifer

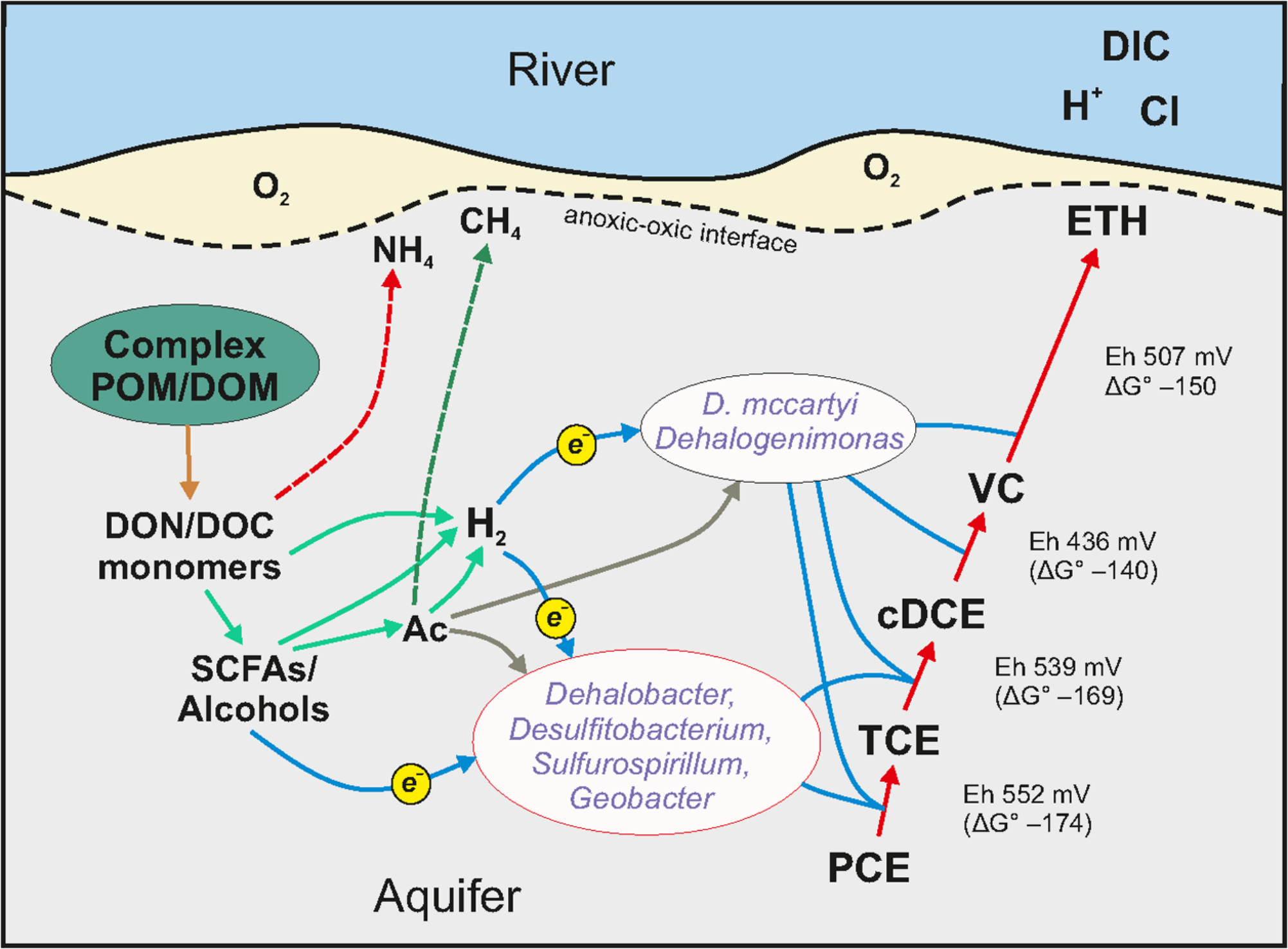
River
DIC
H+ Cl
O2
O2
anoxic-oxic interface
NH4
CH4
ETH
Complex POM/DOM
DON/DOC monomers
SCFAs/ Alcohols
H2
Ac
e-
e-
e-
D. mccartyi Dehalogenimonas
Dehalobacter, Desulfitobacterium, Sulfurospirillum, Geobacter
VC
cDCE
TCE
PCE
Eh 507 mV
ΔG° –150
Eh 436 mV
(ΔG° –140)
Eh 539 mV
(ΔG° –169)
Eh 552 mV
(ΔG° –174)
Aquifer

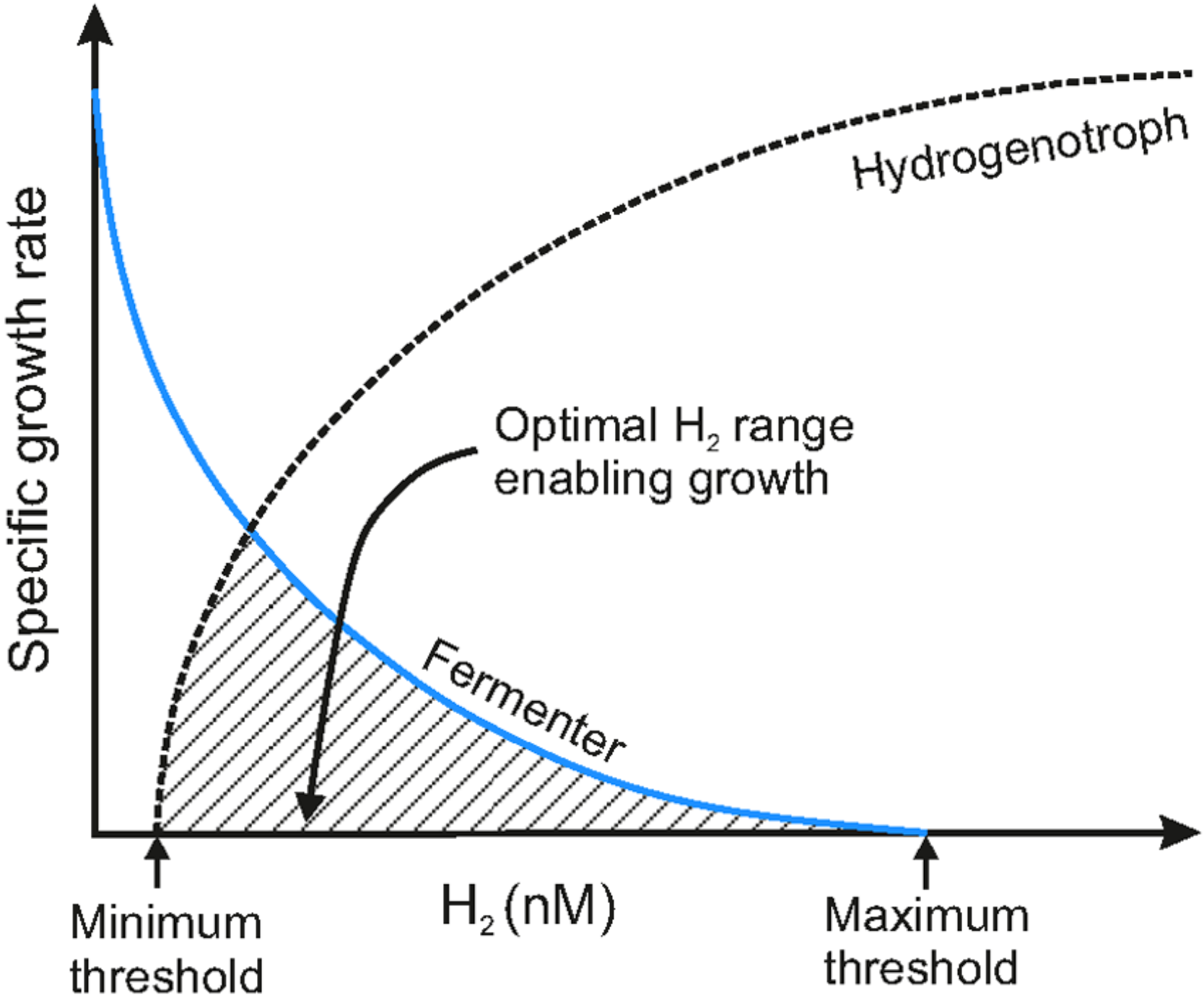
Specific growth rate
Hydrogenotroph
Optimal H_2 range
enabling growth
Fermenter
Minimum
threshold
H_2 (nM)
Maximum
threshold

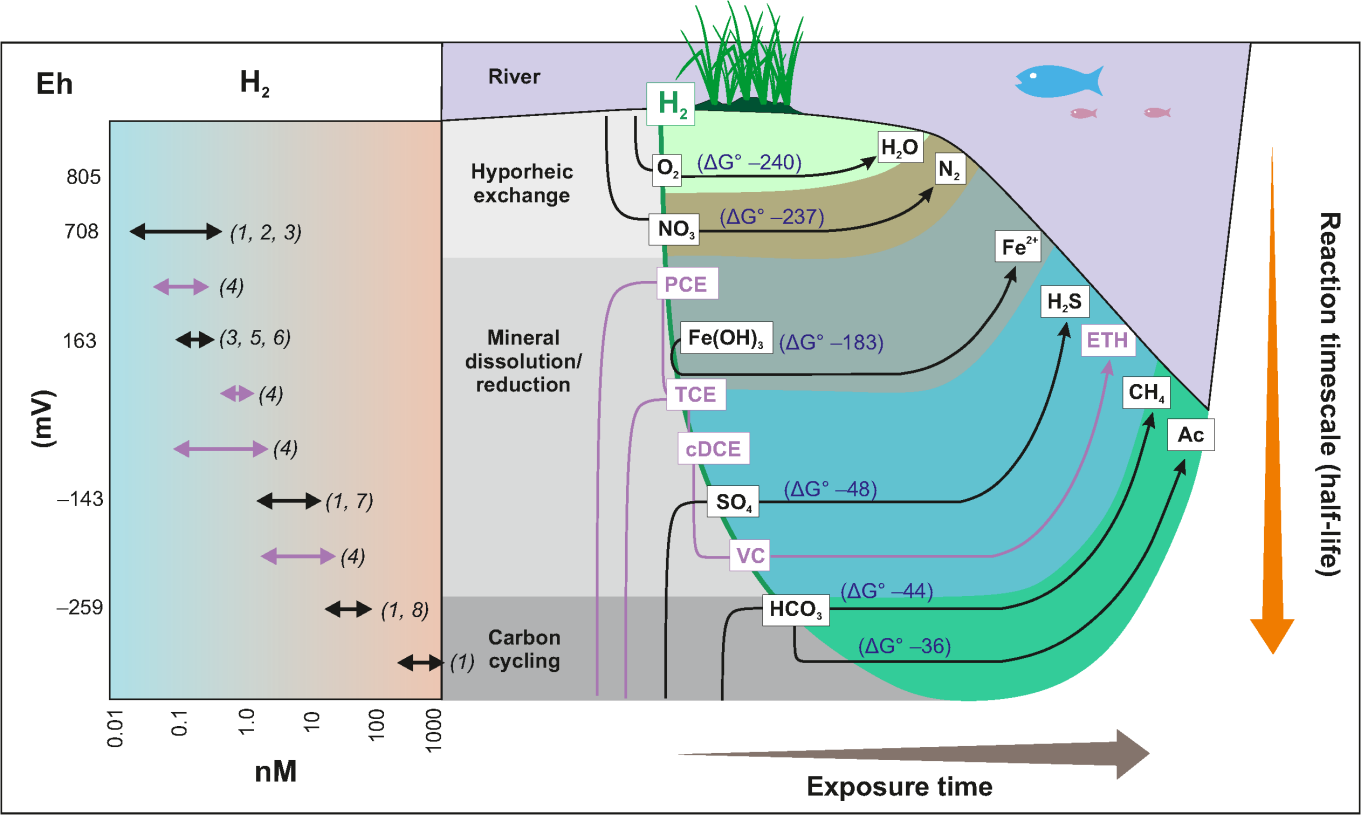
Eh
H2
River
H2
Hyporheic exchange
O2
(ΔG° –240)
H2O
N2
NO3
(ΔG° –237)
Fe2+
PCE
H2S
Mineral dissolution/ reduction
Fe(OH)3
(ΔG° –183)
ETH
CH4
TCE
Ac
cDCE
SO4
(ΔG° –48)
VC
(ΔG° –44)
HCO3
(ΔG° –36)
Carbon cycling
805
708
163
–143
–259
(mV)
(1, 2, 3)
(4)
(3, 5, 6)
(4)
(4)
(1, 7)
(4)
(1, 8)
(1)
0.01
0.1
1.0
10
100
1000
nM
Exposure time
Reaction timescale (half-life)

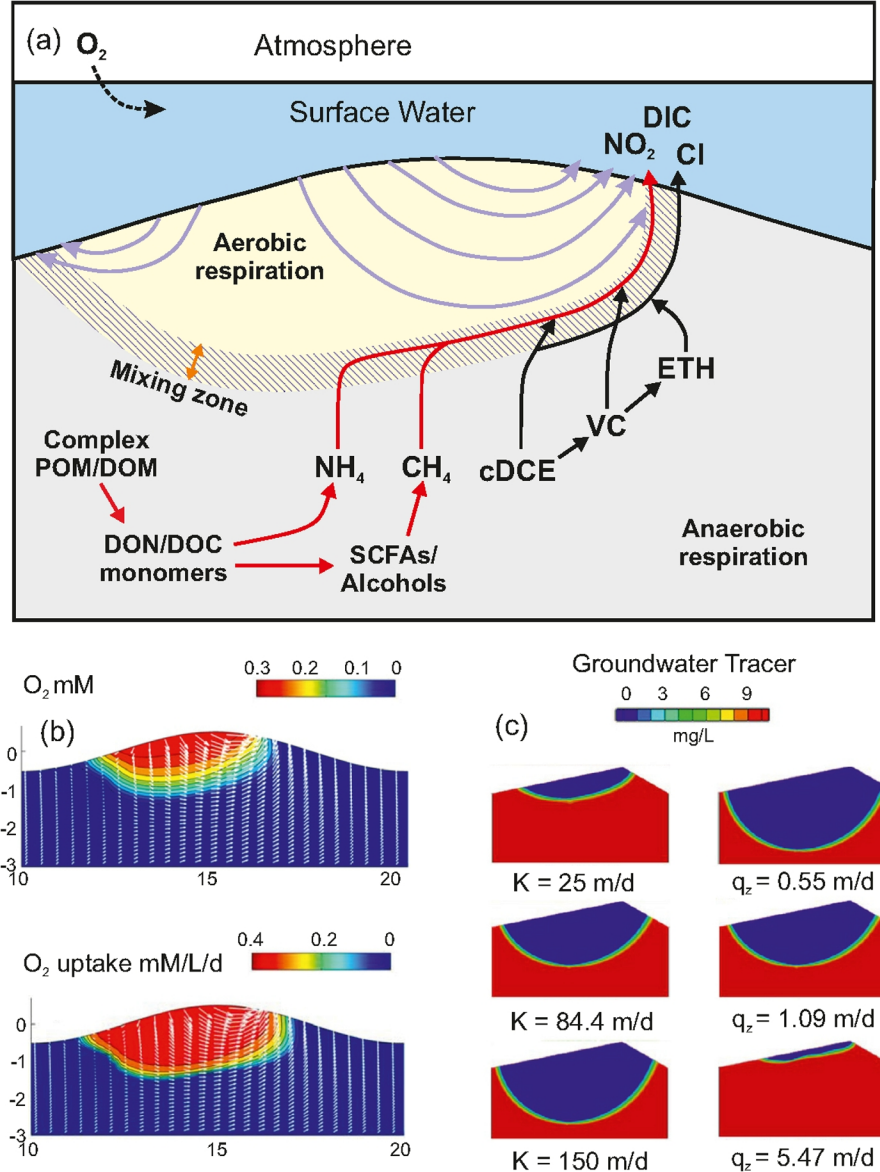
(a)
O2
Atmosphere
Surface Water
DIC
NO2
Cl
Aerobic respiration
Mixing zone
ETH
VC
Complex POM/DOM
NH4
CH4
cDCE
DON/DOC monomers
SCFAs/ Alcohols
Anaerobic respiration
O2 mM
0.3 0.2 0.1 0
(b)
0
-1
-2
-3
10
15
20
O2 uptake mM/L/d
0.4 0.2 0
Groundwater Tracer
0 3 6 9
mg/L
(c)
K = 25 m/d
qz = 0.55 m/d
K = 84.4 m/d
qz = 1.09 m/d
K = 150 m/d
qz = 5.47 m/d

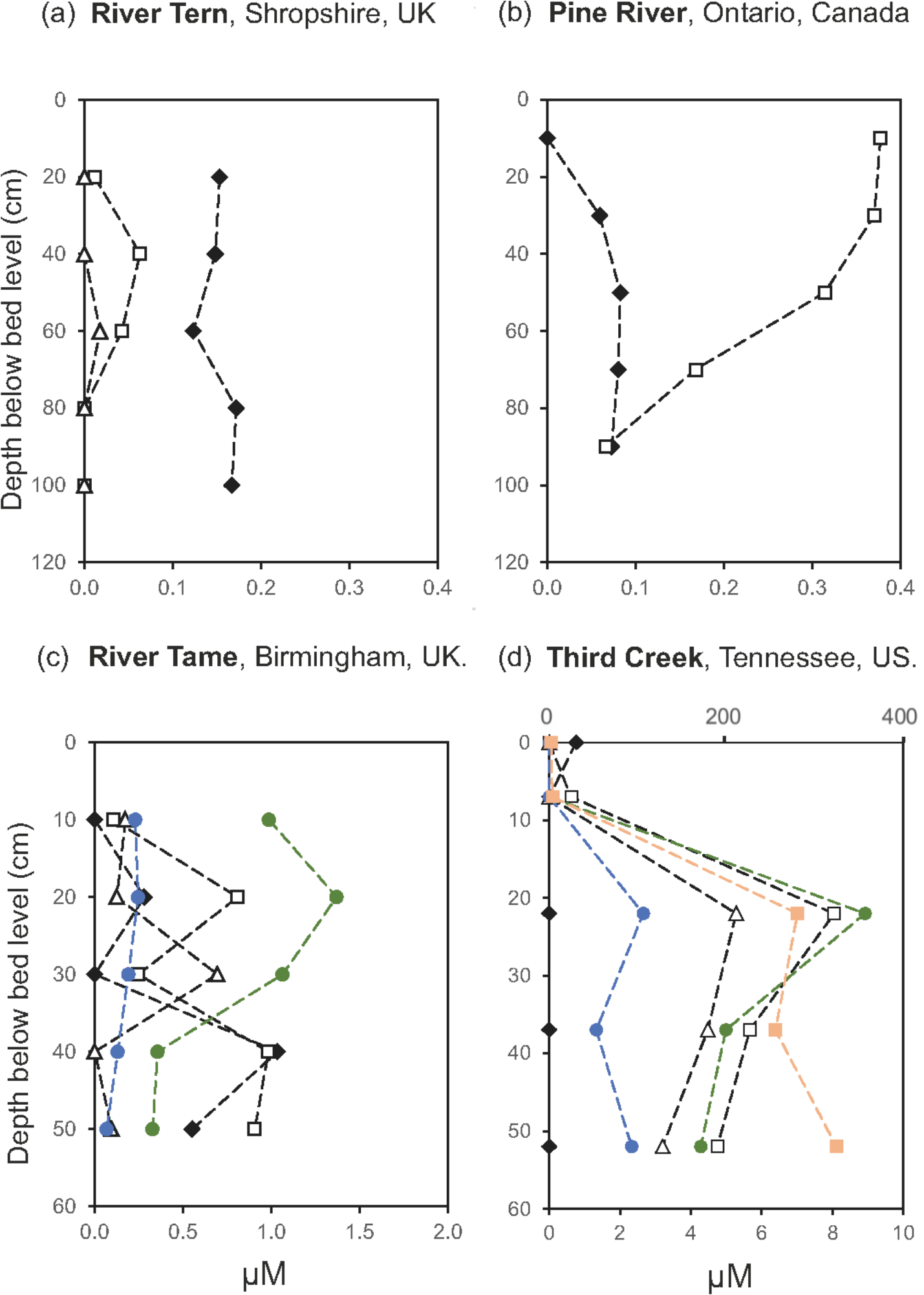
(a) River Tern, Shropshire, UK
(b) Pine River, Ontario, Canada
(c) River Tame, Birmingham, UK.
(d) Third Creek, Tennessee, US.
Depth below bed level (cm)
0
20
40
60
80
100
120
0.0
0.1
0.2
0.3
0.4
10
30
50
0.5
1.0
1.5
2.0
200
400
2
4
6
8
10
μM

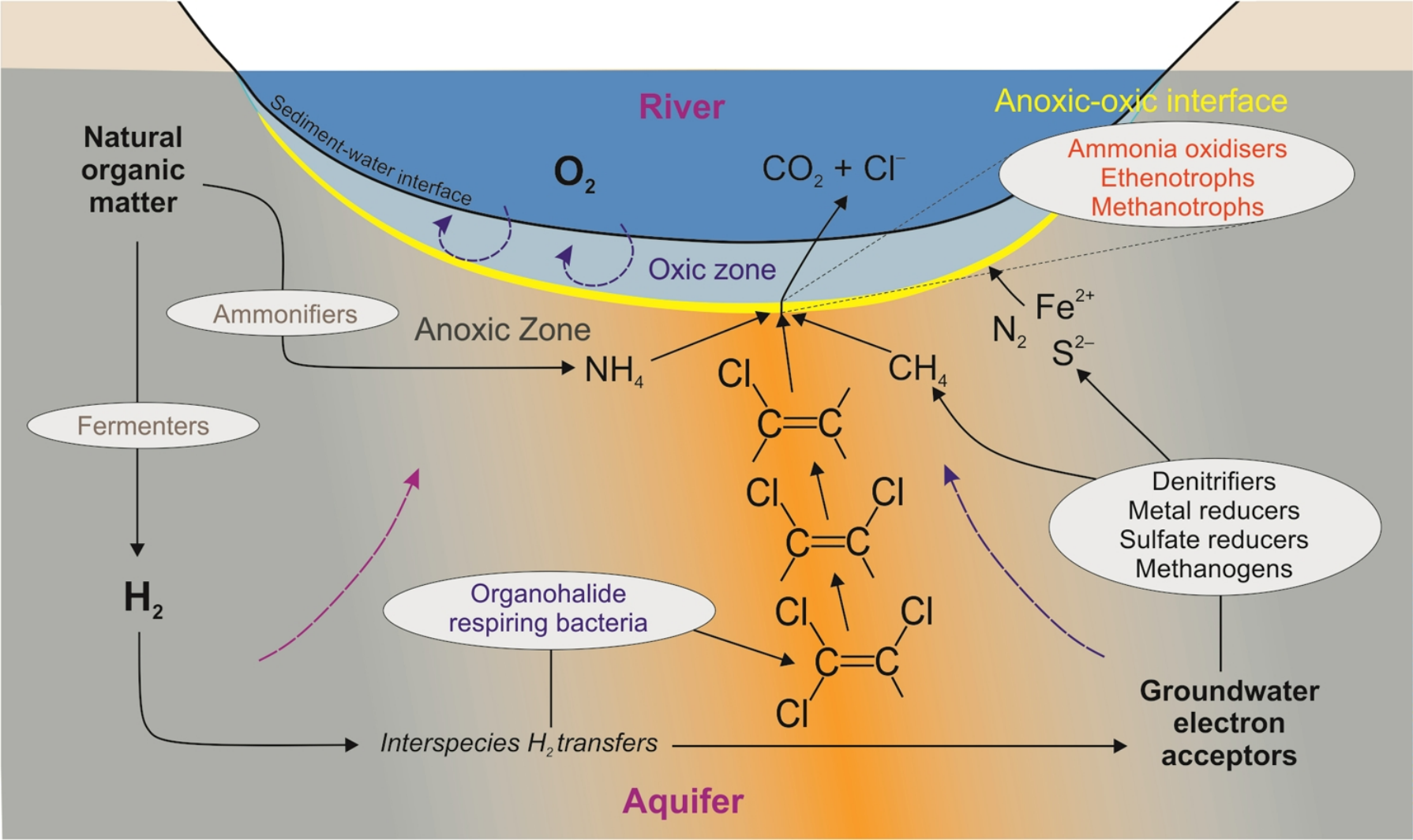
River
Anoxic-oxic interface
Sediment-water interface
Natural organic matter
O_2
$CO_2 + Cl^-$
Ammonia oxidisers
Ethenotrophs
Methanotrophs
Oxic zone
Ammonifiers
Anoxic Zone
NH_4
N_2
Fe^{2+}
S^{2-}
CH_4
Fermenters
Denitrifiers
Metal reducers
Sulfate reducers
Methanogens
H_2
Organohalide respiring bacteria
Interspecies H_2 transfers
Groundwater electron acceptors
Aquifer